REGISTERED No. BG. 315

PROCEEDINGS

OF THE

INDIAN ACADEMY OF SCIENCES

VOL. LIII] *SECTION A* [No. 5

MAY 1961

OF MICHIGAN
AUG 17 1961
PHYSICS LIBRARY

Price Rs. 2 or 3 Sh. *Annual Subscription Rs. 18*

PRINTED AT THE BANGALORE PRESS, BANGALORE CITY, BY T. K. BALAKRISHNAN
SUPERINTENDENT, AND PUBLISHED BY THE INDIAN ACADEMY OF
SCIENCES, BANGALORE

FLUORESCENCE AND SCINTILLATION SPECTRA OF CsI (Tl) CRYSTAL

By R. G. Lagu and B. V. Thosar, F.A.Sc.

(Tata Institute of Fundamental Research, Bombay-5, India)

Received December 19, 1960

Introduction

A single crystal of CsI (Tl) supplied by Harshaw Chemical Co., was studied at room temperature for its luminescence spectra under ultra-violet excitation and scintillation spectra under γ-rays. As pointed out by Sciver W. J. Van,[6] the identity of luminescence centres in the two types of excitation cannot be assumed unless it is established that the emission spectrum in fluorescence under ultra-violet and that in scintillation under γ-rays are the same. There does not seem to be any systematic spectroscopic study of the scintillations excited by γ-rays in Thallium-activated alkali halide crystals, though these crystals are now in constant use for γ-ray scintillation spectrometry. The purpose of these studies was to compare the emission spectra of CsI (Tl) crystal under ultra-violet and γ-ray excitations. If the emission spectrum of scintillations under γ-rays had more than one band, it would be of great interest to determine the decay time and decay characteristics of each of the emission peaks separately. For this reason, it is necessary to measure the emission spectrum of scintillations in some detail. For purposes of comparison, the emission spectra of Thallium-activated CsBr, NaI and KI were also studied.

Experimental Arrangement

A Steinheil 3-prism spectrograph with collimator and camera having apertures $\sim f/3$ and $\sim f/4$ respectively was employed and the spectra in the visible range 4000 Å–6000 Å were photographed on a Kodak Tri-X film. The average reciprocal dispersion of the spectrograph in the visible range was ~ 50 Å/mm. A condenser with an aperture $\sim f/1{\cdot}5$ collected light from the crystal on to the slit of the spectrograph. As the spectra at room temperature were expected to be broad continua and the light output was very low especially with γ-excitation, the slit-width was kept as large as 400 μ. Co^{60} ($\sim$7 m.c.) provided a γ-ray source while suitable filter solutions were employed to cut off visible radiation and transmit mainly ultra-violet from an intense high-pressure quartz mercury lamp. The crystal

was kept in a light-tight housing as exposures of the order of a few days were necessary to obtain spectra under γ-ray excitation.

The liquid filters used with the ultra-violet source were as follows:

(1) ($CoSO_4 + NiSO_4$) solution in water in a quartz cell having a path-length of approximately 2 cm. transmits the radiation between 3600 Å and 2300 Å with a peak transmission of $\sim 75\%$ at 3000 Å. This filter could thus entirely remove the visible continuum in the spectrum of Hg-source and reduce considerably the intensities of lines in the visible region. This was necessary to prevent visible light reflected and scattered from the crystal, masking the genuine luminescence spectrum.

(2) ($I_2 + CCl_4$) in a similar quartz cell transmits between 4400 Å and 3000 Å with a peak transmission of $\sim 60\%$ at 3800 Å.

These filters were employed one at a time between the Hg-source and the crystal. With them, the space in the visible range was made clear, as it were, for the true luminescence spectrum to appear. Duration of exposures required were of the order of a few minutes.

RESULTS

The spectrograms thus obtained were microphotometered on a Hilger non-recording instrument. The results are given in Fig. 1(*a*)–1 (*g*).

The scintillation spectrum of CsI (Tl) excited by γ-rays is continuous between 4000 Å and 6000 Å with at least three peaks at approximately 5950±50 Å, 5700±50 Å and 4750±50 Å. The three peaks are very well pronounced. There is probably a fourth peak at 4400 Å but this is rather doubtful since it appears as a small shoulder to 4750 Å band [Fig. 1 (*a*)]. The luminescence spectrum of CsI (Tl) is described as 'white' by J. B. Birks[5] while the range is given by Hahn and Rossel[4] as 4200–5700 Å.

When fluorescence is excited by ultra-violet light with a continuous range between 2300 Å and 3600 Å, the emission spectrum is continuous with peaks at identical wavelengths as in scintillation spectrum. These peaks, however, are not as well resolved as in γ-ray excitation experiment [Fig. 1 (*b*)]. With the exciting spectrum comprising of wavelengths between 3000 Å and 4400 Å, only a part of the emission spectrum appears, *i.e.*, only the wavelengths greater than 5600 Å are excited. Nevertheless, in this region the yellow bands appear again at identical positions as with γ-ray or deep ultra-violet excitation [Fig. 1 (*c*)]. These two peaks are certainly more prominent than in Fig. 1 (*b*).

Conclusions

The fluorescence and scintillation spectra for CsI (Tl) show emission bands centred around the same wavelengths. This experimental observation indicates that the fluorescence and scintillation centres are one and

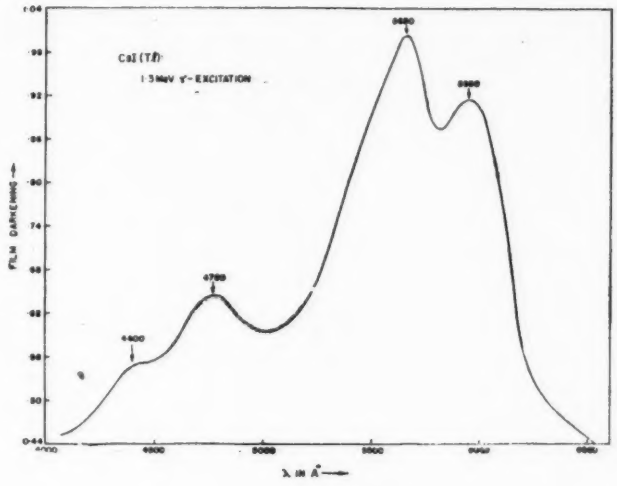

Fig. 1 (*a*)

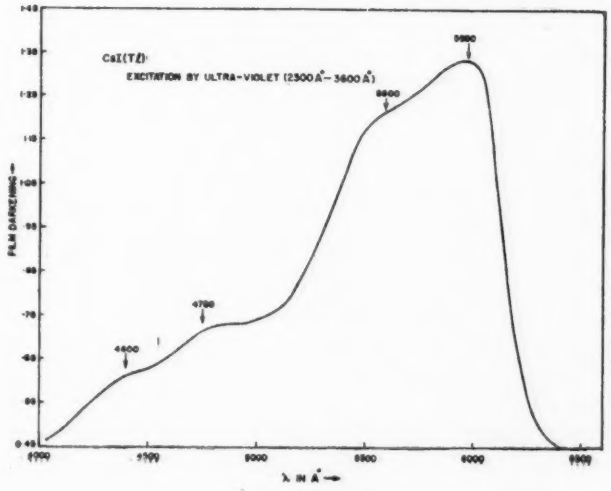

Fig. 1 (*b*)

the same. The same fact was also observed for NaI (Tl) and KI (Tl) crystals.

Comparison of Fig. 1 (*b*) and 1 (*c*) shows that only a part, *i.e.*, the longer wavelength portion, of the emission spectrum is excited by ultra-violet

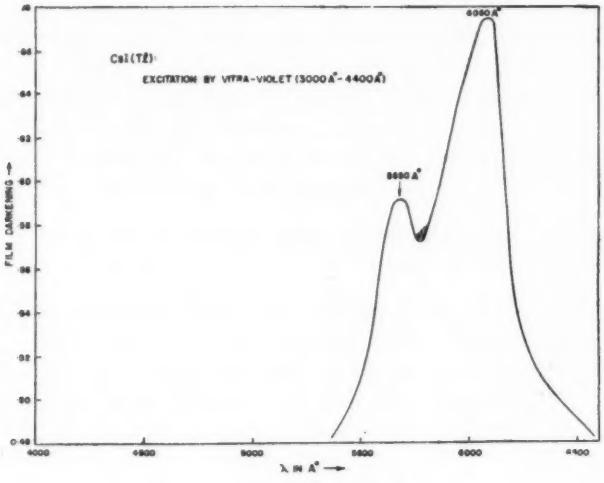

FIG. 1 (*c*)

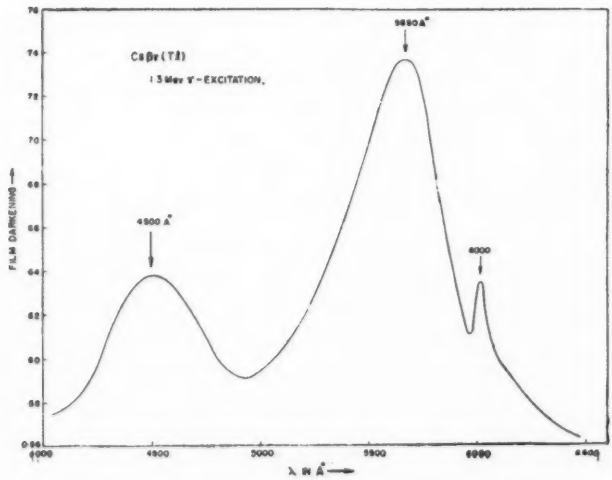

FIG. 1 (*d*)

light transmitted by $I_2 + CCl_4$) filter, while the complete spectrum appears with ($NiSO_4 + CoSO_4$). Hence, the luminescence in the range of wavelengths less than 5600 Å is excited by the wavelengths between 2300 Å and 3000 Å. The experiments with monochromatic ultra-violet excitation would

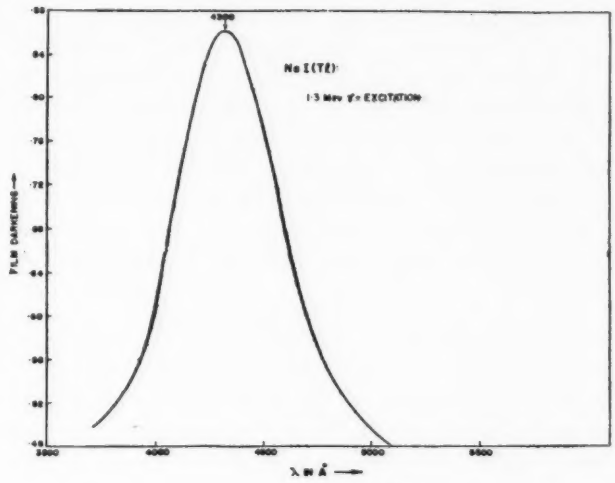

FIG. 1 (*e*)

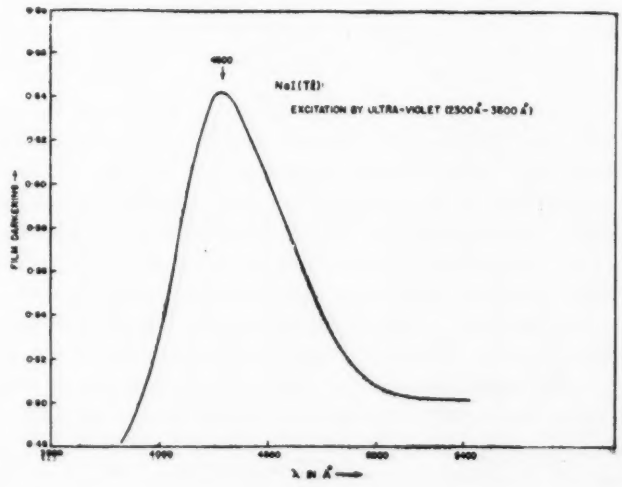

FIG. 1 (*f*)

probably yield the wavelength at which λ 4750Å band begins to appear. Thus, the transition energy of the excited state responsible for 4750 Å band would be obtained. Some calculations of the shapes of the potential energy curves for the ground and the excited states to account for the transition energy, so obtained, could then be attempted.

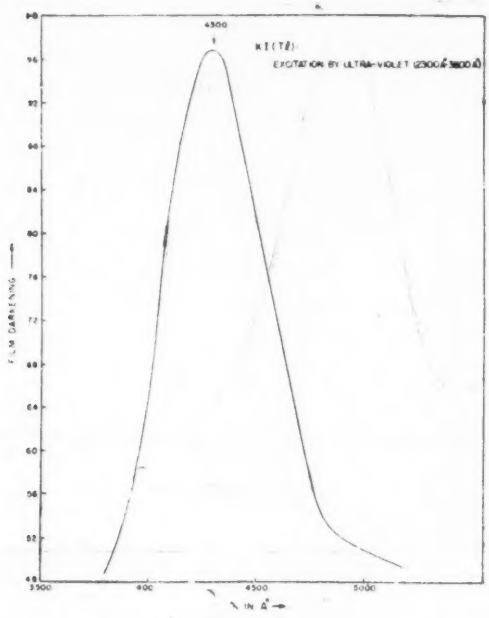

FIG. 1 (g)

As only the yellow bands can be excited by wavelength greater than 3000 Å while the λ 4750 Å band appears when the shorter wavelengths are present in the exciting spectrum, it can be suggested that the excited state for the yellow emission lies in between that for 4750 Å emission and the ground state. It is, of course, assumed that all the optical transitions belong only to one type of luminescence centre, presumably Tl^+ substituting Cs^+. The transition energies corresponding to 5800 Å and 4700 Å emission are roughly 2·1 ev. and 2·6 ev. respectively. The absorption data for CsI (Tl) as given by Pringsheim[1] consists of three peaks centred at 2990 Å, 2690 Å and 2410 Å. The transition energies corresponding to these three peaks are approximately 4·14 ev., 4·6 ev. and 5·14 ev. respectively. Our experiments indicate that the absorption of 2990 Å is responsible for the luminescence emission in the yellow region, with about 2 ev. dissipated in the

crystal corresponding to one yellow photon emission. The correlation between λ 4700 Å emission and the absorption can be established only with the monochromatic ultra-violet excitation experiments.

When Fig. 1 (*a*) is compared with Fig. 1 (*d*), we find that the emission spectrum of CsI (Tl) shows a remarkable similarity to that of CsBr (Tl), although the latter shows a peak at 4500 Å instead at 4750 Å. Also from Fig. 1 (*f*) and Fig. 1 (*g*), we observe that the emission of NaI (Tl) is almost identical with that of KI (Tl) under ultra-violet excitation both showing a single band centred at 4300 Å. Incidentally, this value agrees fairly well with those given by Birks as 4100±400 Å for NaI (Tl) and 4100±450 Å for KI (Tl) and also with the values reported by Milton and Hofstadter[3] as 4100±850 Å for NaI (Tl) and 4000±600 Å for KI (Tl) under γ-ray excitation from Ra source.

We note that CsI (Tl) and CsBr (Tl) have a b.c.c. lattice while NaI (Tl) and KI (Tl) are f.c.c. With high concentration of Tl, KCl (Tl) which is also f.c.c. emits a band at 4700 Å.[2] In spite of these differences in details, it appears that the essential structure of the luminescence spectrum depends upon the type of crystal lattice or more precisely on the number and disposition of the nearest neighbours of the substitutional Tl^+ ion. The small differences in the position of the peaks may be attributed to the types, symmetry and distances of perturbing ions.

Summary

Fluorescence and scintillation spectra of a single crystal of CsI (Tl) at room temperature excited by ultra-violet (with $\lambda = 2300$ Å–3600 Å) and γ-rays from Co^{60} respectively are presented. They are continuous in the visible region (4000 Å–6000 Å) with at least three well-pronounced peaks at 5950±50 Å, 5700±50Å and 4750±50 Å. There is an indication of a fourth peak at 4400 Å. The same peaks appear in both types of excitation. Hence the luminescence centres in the two processes seem to be identical. With the exciting ultra-violet comprising of $\lambda > 3000$ Å, only the two peaks in yellow region appear. Hence, it seems that the excited level responsible for the yellow emission lies in between the ground and the excited state responsible for 4750 Å emission. Luminescence spectra for CsBr (Tl), NaI (Tl) and KI (Tl) are also presented. It is concluded from the comparison of all the spectra obtained that the type of emission spectrum depends on the crystal structure.

ACKNOWLEDGEMENT

The authors wish to thank Professor R. K. Asundi and other members of the Spectroscopy Group in Analytical Division of the Atomic Energy Establishment, Trombay, for the use of their spectroscopic instruments and helpful discussions.

REFERENCES

1. P. Pringsheim .. *Fluorescence and Phosphorescence*, Interscience Publishers Ltd., London, 1949, 619.
2. ———— .. *Ibid.*, 1949, 620.
3. Milton and Hofstadter .. *Phys. Rev.*, 1949, **75**, 1289.
4. Unpublished data of Bonanomi and Rossel quoted by B. Hahn and J. Rossel, *Helv. Phys. Acta*, 1953, **26**, 276.
5. Birks, J. B. .. *Scintillation Counters*, Pergamon Press Ltd., London, *Electronics and Waves Monographs*, 1953, **57**.
6. Van Sciver, W. J. .. *L'electronique Nucleaire*, Proceedings of the International Symposium on Nuclear Electronics organized by the French Society of Radioelectricians, Paris, 1959, **1**, 37.

A STUDY OF THE PRE-SUNRISE F-LAYER STRATIFICATION AT KODAIKANAL

By B. N. Bhargava and R. V. Subrahmanyan

(Astrophysical Observatory, Kodaikanal)

Received October 21, 1960

(Communicated by Dr. M. K. Vainu Bappu, F.A.Sc.)

Abstract

The pre-sunrise phenomenon of a rapid drop in the maximum ionic density of F-layer followed by an increase in the semi-thickness and height of the layer and stratification is described. The phenomenon, which is found to occur prominently during periods of low or moderate solar activity and during winter months, is discussed in relation to the distortion of the overhead Sq. current system and vertical drift of ionization.

1. Introduction

Vertical soundings of the ionosphere using a N.B.S. type C–3 Ionosonde were started at Kodaikanal (Latitude, 10° 14′ N., Longitude 77° 28′ E.) early in 1952. The early morning phenomenon of F-layer stratification was observed soon after and was reported, on the basis of preliminary observations, by one of the present authors (1952). Similar observations have been made by Bandyopadhyaya (1959) at Haringhata near Calcutta and have been discussed for possible bearing on the E-layer cusps observed there. Round-the-clock observations at Kodaikanal were commenced in September 1955 and intensive observations were made during the 3-hour period preceding sunrise in order to determine the nature of the stratification which was frequently observed during periods of low solar activity and during winter.

2. Effect of Vertical Drift on Electron Density

The basic continuity equation of electron density N in a simple solar-controlled region is

$$\frac{\partial N}{\partial t} = q(t) - \alpha N^p - \text{div. } (Nv) \qquad (1)$$

where $q(t)$ represents the ion production term and αN^p is the electron dissipation rate, p being the exponent to indicate whether the dissipation process is one of recombination ($p = 2$) or of attachment ($p = 1$). The term div. (Nv) represents the electron transport rate.

If we restrict our attention to the peak of the layer, Equation (1) reduces to

$$\frac{\partial N}{\partial t} = q(t) - \alpha N^p - N_m \frac{\partial v}{\partial z} . \tag{2}$$

Martyn (1947 *a*, *b*, 1948) had indicated that vertical movements may cause important perturbations in an ionized region. Appleton and Lyon (1955) have discussed the effects of vertical drift in distorting the electron density profile of a Chapman-like region. They have shown that the fractional change in the level of maximum electron density $\delta h(N_m)$ and in its magnitude δN_m due to vertical drift are given by

$$\left.\begin{aligned} \delta h(N_m) &= \frac{v}{2\alpha N_m} && \text{(recombination)} \\ \delta h(N_m) &= \frac{v}{\beta} && \text{(attachment)} \end{aligned}\right\} \tag{3}$$

$$\left.\begin{aligned} \frac{\delta N_m}{N_m} &= -\frac{1}{2\alpha N_m} \cdot \frac{\partial v}{\partial h} - \frac{1}{4H^2}\left(\frac{v}{2\alpha N_m}\right)^2 && \text{(recombination)} \\ \frac{\delta N_m}{N_m} &= -\frac{1}{\beta} \cdot \frac{\partial v}{\partial h} - \frac{1}{2H^2}\left(\frac{v}{\beta}\right)^2 && \text{(attachment)} \end{aligned}\right\} \tag{4}$$

where α and β are recombination and attachment coefficients respectively, v is the vertical drift velocity reckoned positive upwards, $(\partial v/\partial h)$ is its vertical gradient and H is the scale height of the ionized constituent. Equations (3) and (4) indicate that the influence of vertical drift on N_m and its height is determined by drift characteristics and by the quantity $(1/2\alpha N)$ or $(1/\beta)$.

3. Changes in F-Layer before Sunrise

As stated previously, the early morning hours of winter months, particularly during periods of low solar activity, are characterised by rapid changes of maximum ionic density, height and layer shape. A typical sequence of ionograms observed between 0430 and 0630 hours on the morning of January 4, 1960, is given in Fig. 1 (Plate VII). The layer is normal till about 0430 hours. Shortly afterwards, the ionic density begins to drop and the virtual height registers an increase. Around 0600 hours the critical frequency of

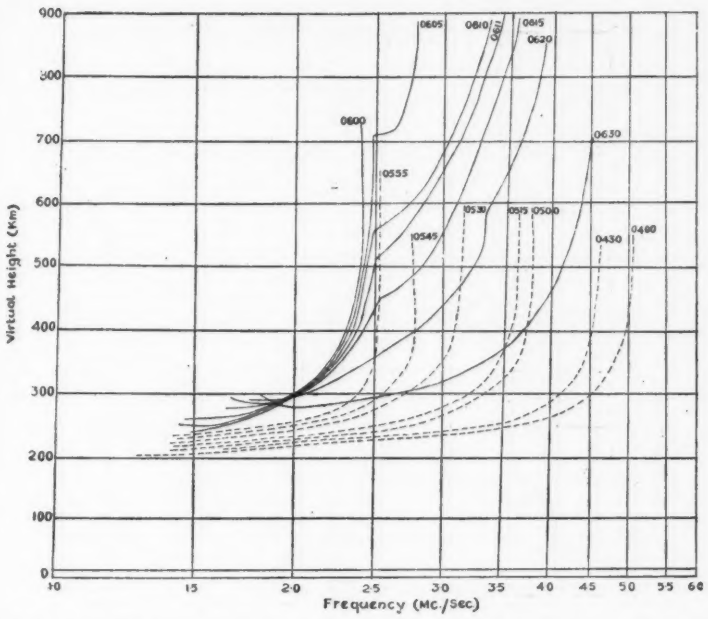

FIG. 2. Ordinary component of the *h'-f* traces between 0400 hr. and 0630 hr. I.S.T. on January 4, 1960.

about 2·5 Mc./sec. is registered and rapid changes in the structure of the layer are noticed. The layer is stratified and the two strata become well defined. Thereafter, the maximum electron densities in both the layers increase and the two layers merge. The layer becomes normal by about 0630 hours. These changes are shown in Fig. 2 where the ordinary components of the *h'-f* traces between 0400 and 0630 hours are reproduced.

4. The Distribution of Electron Density as a Function of True Height

In order to examine the variations of electron densities at several levels, the *h'-f* records during the interval 0330 hours to 0630 hours for two typical days, January 12, 1956 and January 4, 1960, were reduced to $(N, h)_t$ profiles using Tables of Coefficients given by Schmerling and Ventrice (1959). The profiles for January 12, 1956 and January 4, 1960, are given in Fig. 3 *a* and Fig. 3 *b* respectively. From the $(N, h)_t$ profiles for one of these days, *viz.*, January 4, 1960, the height variations of constant ionization levels were deduced and the resulting curves are presented in Fig. 4. It will be seen

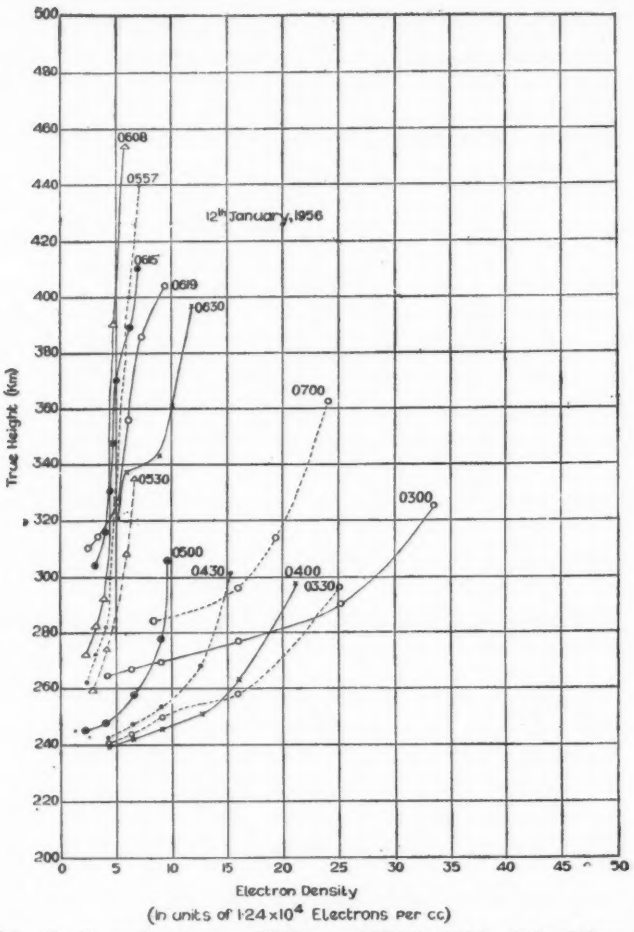

FIG. 3 (*a*). (N, *h*)$_t$ profiles between 0300 hr. and 0700 hr. I.S.T., deduced from *h'-f* records of January 12, 1956.

from the curves of Fig. 3 *a* and Fig. 3 *b* that considerable variations in height and thickness occur near the layer peak from 0430 hours and these variations are maximum around 0600 hours. Fig. 4 shows some interesting features. Perturbations in the heights at different ionization levels take place. At 0600 hours when the layer gets stratified, the variations in height appear to be maximum. It is also noticed that the layer appears to rise as a whole with a velocity of about 100 km./hr. Simultaneously, the critical

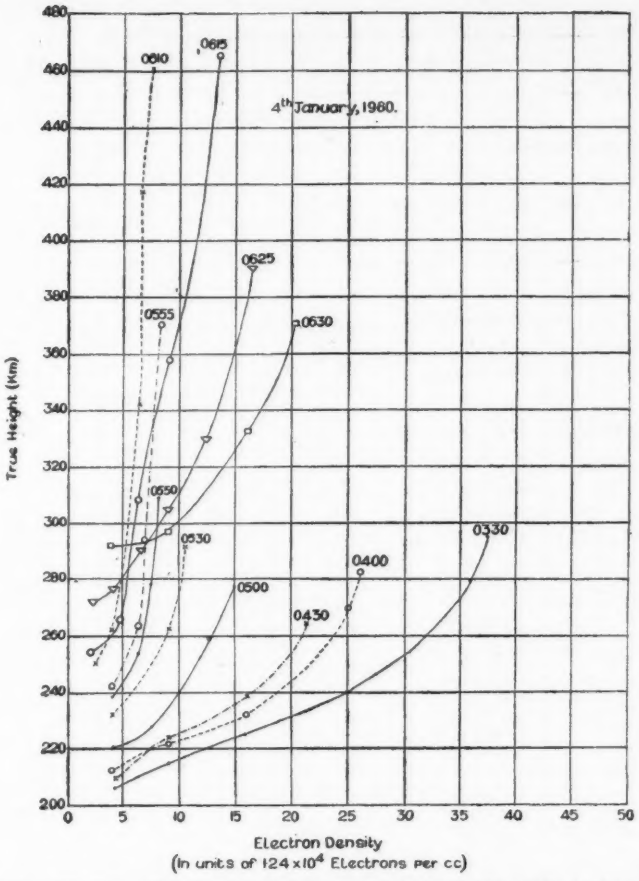

FIG. 3 (*b*). (N, h)$_t$ profiles between 0330 hr. and 0630 hr. I.S.T., deduced from h'-f records of January 4, 1960.

frequency drops to a low value of about 2·5 Mc./sec. at the time of stratification.

5. DISCUSSION

(i) *Changes in the layer shape due to vertical movements.*—As mentioned earlier, the effect of vertical drift velocity is to perturb the ionized layer, the electron density changes being represented by the continuity equation (1). It will be further seen from the Appleton and Lyon equation (4) that irrespective of its sign, the effect of drift velocity v will be to spread out the ionization. The rise or fall in height of peak ionic density will depend upon the

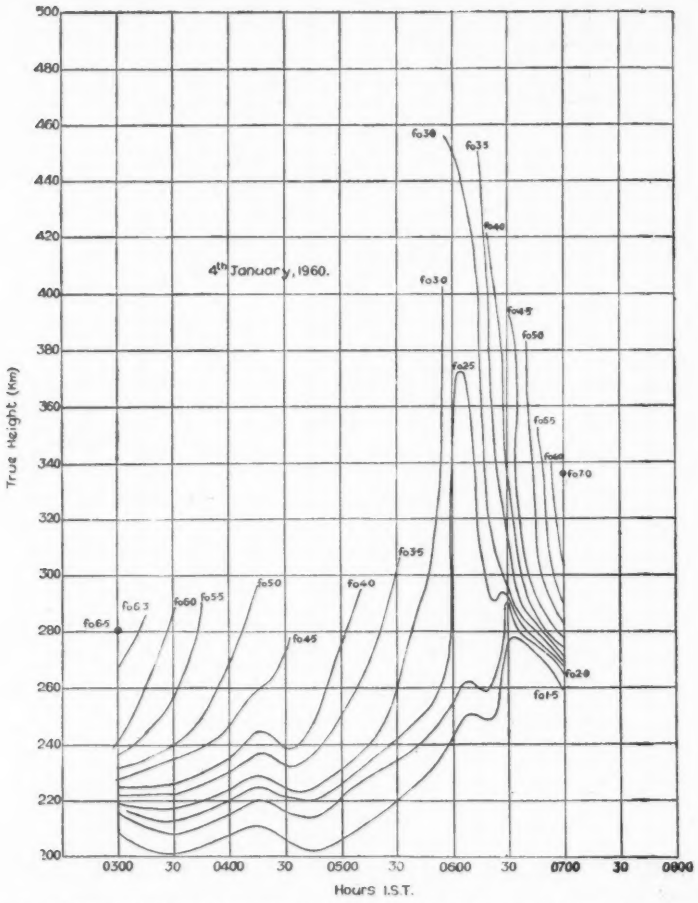

FIG. 4. Height variations of constant ionization levels of January 4, 1960, during pre-sunrise F-region "splitting".

sign of v, equation (3). The magnitude and sign of the gradient of drift velocity will determine the overall effect of distortion on peak ionic density.

Using the electron density-height profiles the time variation of the heights of peak ionic density was obtained. It was found that the peak rises rapidly from 270 km. at about 0430 hours to over 450 km. at 0600 hours.

According to Martyn (1955), the effect of height gradient of electron loss ($\partial\alpha/\partial z$) is to move the level of Z_m upwards. It can be seen from

the constant ionization levels (Fig. 4) that just before sunrise, the level of Z_m is very much lifted up, indicating thereby, that the magnitude of $(\partial a/\partial z)$ is very much increased.

Following Martyn, we shall write

$$a = a_0 e^{-z/a} \tag{5}$$

Differentiating the above, we get

$$\frac{\partial a}{\partial z} = -\frac{a}{a}. \tag{6}$$

If the magnitude of $(\partial a/\partial z)$ is large, the value of "a" should be small. This can be examined in a different way. Following Marasigan (1958), we may write that at the point of inflexion

$$\frac{\partial}{\partial z}(aN^p) = 0. \tag{7}$$

Differentiating (7) we get

$$\frac{\partial a}{\partial z} = -\frac{a}{N^p} \cdot \frac{\partial}{\partial z}(N^p). \tag{8}$$

From (6) and (8) we get

$$a = \frac{N}{p\left(\frac{\partial N}{\partial z}\right)}$$

$$= \frac{N}{\left(\frac{\partial N}{\partial z}\right)} \quad (p = 1, \text{ attachment process}).$$

It is an observed fact that just before sunrise the magnitude of N is very much reduced while $(\partial N/\partial z)$ is much increased, thereby indicating a small value for "a" just before splitting. It appears, therefore, that the large upward shift in the level of maximum ionization is followed by splitting of the layer due to large value of height gradient of loss coefficient $(\partial a/\partial z)$.

(ii) *Magnitudes of vertical drift velocity v and its gradient* $(\partial v/\partial z)$.— Using the relation $\delta h(N_m) = (v/\beta)$ where β is the attachment coefficient, values of v were computed at 10 minutes intervals on January 4, 1960. Substituting these values of v in the continuity equation, the magnitude and sign of $(\partial v/\partial z)$ at the height of maximum ionization at the same intervals were also computed. These values are given in Tables I *a* and I *b*.

TABLE I (*a*)

Time I.S.T.	Magnitude of drift velocity gradient ($\partial v/\partial z$) on January 4, 1960, in sec.$^{-1}$ at 10-minute interval
	$10^{-5}\times$
0400	−14·9
10	−13·5
20	−11·5
30	−13·1
40	−19·4
50	−18·4
0500	−16·8
10	−15·2
20	−13·5
30	−11·7
40	− 9·5
50	− 6·1
0600	− 2·9

It will be seen that starting from about 0440 hours v was positive and its magnitude increased rapidly. At the same time ($\partial v/\partial z$) approached zero, starting from a negative value, thereby indicating that the second term of the right side of the equation

$$\frac{\delta N_m}{N_m} = -\frac{1}{\beta}\cdot\frac{\partial v}{\partial z} - \frac{1}{2H^2}\left(\frac{v}{\beta}\right)^2$$

was predominant in determining the electron density changes at the peak.

(iii) *Distortion of the Sq. current system and the associated movements.*— Martyn and others (1952) have indicated that the morphology of the F-region may be profoundly affected by the events in the E-region because

TABLE I (*b*)

Time I.S.T.	Magnitude of drift velocity v in units of 10^3 m. sec.$^{-1}$ on January 4, 1960, at 10-minute interval
0400	−1·95
10	−1·45
20	−0·80
30	+0·60
40	+0·95
50	+1·27
0500	+1·42
10	+1·50
20	+1·66
30	+2·00
40	+2·60
50	+4·40
0600	+3·52

the electric fields would be communicated to F-region along the lines of magnetic force. This is supported by the experiments of Maple, Bowen and Singer (1952) and more recently by those of Van Allen and Cahill (1958) which indicate that the E-region is the seat of strong electric currents and that these currents are responsible for the diurnal quiet-day Sq. variations of the magnetic elements. Any change in the horizontal intensity at low latitude stations, therefore, indicates a distortion of the Sq. current intensity, the magnetic field being related to the electric field by

$$\Delta H = 2\Pi I = 2\Pi K \Delta E. \qquad (9)$$

Further, the magnitude of the drift velocity v is determined by the east-west component of the Sq. current and the strength of the horizontal component of the earth's field.

In order to examine the relationship between the abnormal rise in the peak of electron density in the pre-dawn period and any distortion in the Sq. current intensity, the following analysis was undertaken. Thirty days in January, 1960, for which complete data were available were grouped into two categories depending upon whether the F-layer critical frequency immediately preceding sunrise was below or above an arbitrarily chosen value of 3·0 Mc./sec. There were nine days of the first category and twenty-one days of the second. The departures ΔfoF2 from mean values for these days were derived at half hour intervals between 0300 and 0700 hours I.S.T. Likewise, the departure ΔH in gammas in horizontal force recorded at Kodaikanal were also obtained for the two groups of days at half hour intervals. These departures ΔfoF_2 and ΔH are plotted in Fig. 5. It can be seen at once that on nine days when foF_2 is negative, ΔH is also negative, the maximum dip in ΔfoF2 occurring at about 0600 hours, about an hour and a half later than the dip in ΔH. It is interesting to note that it is just about 0430 hours when the maximum dip occurs in H, that the height-changes in F-layer begin to take place (Figs. 4 and 5) presumably due to distortion of the Sq. current intensity in the dynamo region. The maximum departure in foF2 occurs after an interval of about an hour and a half which is very close to the relaxation time $[\tau = (1/2\alpha N_m)]$ where α is the effective loss coefficient taking into account the vertical drift

$$\left(\alpha_{eff.} = \alpha_0 + \frac{1}{N_m} \cdot \frac{\partial v}{\partial h}\right).$$

It, therefore, appears that the abnormal rise of the layer in the pre-dawn period is associated with the additional movement in the region caused by the distortion in the Sq. current intensity.

(iv) *Influence of solar activity on the occurrence of the pre-sunrise phenomenon.*—The pre-dawn increase in the height of the F-layer and the associated splitting were rarely seen during 1957–59, a period of high solar activity. It is known that the rate of ion production is in general proportional to the intensity of solar ionizing radiation. The magnitude of the first two terms on the right side of the continuity equation (1) will be large as compared to the last term and the effect of the transport term div. (Nv) is likely to be small. Further, at sunspot maximum there may exist (Allen, 1953) a high resistance to movements due to electric or magnetic damping by the higher electric conductivity. The contribution of the movements to the rate of change of ionization becomes progressively smaller with increasing solar activity while the residual overnight ionization densities are comparatively

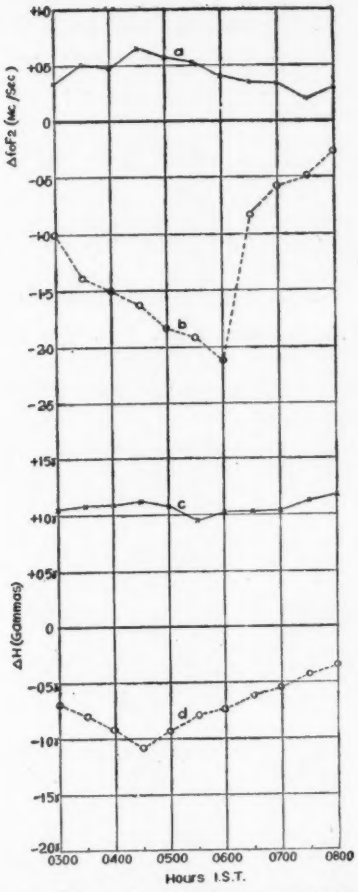

FIG. 5. Upper curves: Variation of Δ foF2 for January 1960: (*a*) for 21 days when pre-sunrise minimum of foF2 was $>3{\cdot}0$ Mc./sec. and (*b*) for 9 days when the parameter was found to be $<3{\cdot}0$ Mc./sec.

Lower curves: Variation of ΔH at Kodaikanal for January 1960, averaged for the same days as in the upper curves (*a*) and (*b*).

much larger. The conditions favourable for bifurcation are, therefore, not fulfilled during the periods of high solar activity.

REFERENCES

1. Allen, C. W. .. *J. Atmosph. Terr. Phys.*, 1953, **4**, 53.
2. Appleton, E. V. and Lyon, A. J. *The Physics of the Ionosphere*, Phys. Soc. Report, 1955, p. 20.

3. Bhargava, B. N. .. *Nature, Lond.*, 1952, **170**, 983.

4. Bandyopadhyaya .. *J. Atmosph. Terr. Phys.*, 1959, **16**, 84.

5. Martyn, D. F. .. *Proc. Roy. Soc.*, 1947 (*a*), **189**, 241.

6. ———— .. *Ibid.*, 1947 (*b*), **190**, 273.

7. ———— .. *Ibid.*, 1948, **194**, 429 and 445.

8. ———— .. *Proc. Conf. Ionosph. Phys.*, Edited by Katz, L. and Gerson N. C. (Part B), 1952, p. 69.

9. ———— .. *The Physics of the Ionosphere*, Phys. Soc. Report, 1955, p. 214.

10. Marasigan, V. .. *J. Atmosph. Terr. Phys.*, 1958, **13**, 107.

11. Maple, E., Bowen, W. A. and Singer, S. F. *Nature, Lond.*, 1952, **170**, 1093.

12. Schmerling, E. R. and Ventrice, C. A. *J. Atmosph. Terr. Phys.*, 1959, **14**, 249.

13. Van Allen, J. A. and Cahill, L. J. *J. Geophys. Res.*, 1958, **63**, 270.

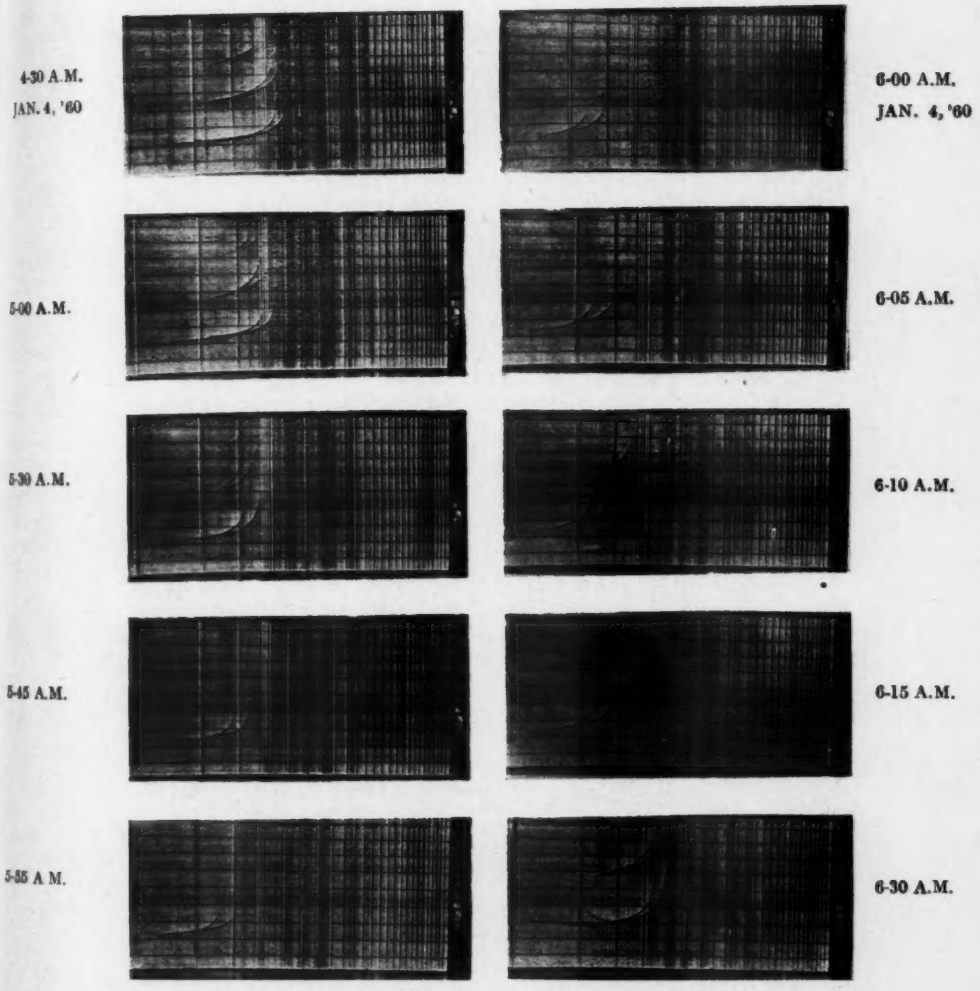

FIG. 1. A sequence of ionograms (January 4, 1960) illustrating the development of pre-sunrise F layer "splitting".

ON THE RELATIVE EXTREMA OF THE TURAN EXPRESSION FOR BESSEL FUNCTIONS

By S. K. Lakshmana Rao

(*Department of Applied Mathematics, Indian Institute of Science, Bangalore-12*)

Received October 27, 1960

(Communicated by Professor B. S. Madhava Rao, F.A.SC.)

Some years ago Otto Szász[1] showed that the Bessel function $J_n(x)$ satisfies the inequality

$$\Delta_n(x) \equiv [J_n(x)]^2 - J_{n+1}(x)\, J_{n-1}(x) \geq \frac{1}{n+1}\,[J_n(x)]^2,$$

$$n \geq 0, \quad x \text{ real} \tag{1}$$

wherefrom he deduced the interesting inequality

$$\Delta_n(x) > 0 \quad \text{for} \quad n > 0, \quad x \text{ real}. \tag{2}$$

The Turán inequality (2) for the function $J_n(x)$ is an immediate consequence of the identity[2]

$$\Delta_n(x) = \frac{4}{x^2} \sum_{k=0}^{\infty} (n + 2k + 1)\left(J_{n+2k+1}(x)\right)^2 \tag{3}$$

which represents $\Delta_n(x)$ as a series of positive quantities whenever $n \geq -1$. V. R. Thiruvenkatachar and T. S. Nanjundiah[3] obtained a new positive representation for $\Delta_n(x)$ by proving the identity

$$\Delta_n(x) = \frac{1}{n+1}\left(J_n(x)\right)^2 + \frac{2}{n+2}\left(J_{n+2}(x)\right)^2$$

$$+ 2n \sum_{k=2}^{\infty} [(n+k-1)(n+k+1)]^{-1}\left(J_{n+k}(x)\right)^2 \tag{4}$$

and the above result (1) of Otto Szász follows from this immediately.

While the above representations for $\Delta_n(x)$ are quite interesting we may also proceed to deduce the inequality (2) by considering the behaviour of the function $\Delta_n(x)$ itself. This procedure leads to several questions concerning the sequences of relative maxima and minima of $\Delta_n(x)$ and the

* Present address: Regional Engineering College, Warangal (A.P.), India.

aim of the present note is the study of these sequences. We prove in particular (Theorem 4 below) that the r-th relative maximum of $\triangle_n(x)$ is larger than the r-th relative maximum of $\triangle_{n+1}(x)$, for any fixed value of r. This answers the question first raised by John Todd for the classical orthogonal polynomials and settled for the Hermite function $H_n(x)$ by Otto Szász[4] and for the Turán expression for the Hermite function by the author.[5]

THEOREM 1: When $n > 0$, the relative maxima of $\triangle_n(x)$ occur at the zeros of $J_{n-1}(x)$ and the relative minima occur at the zeros of $J_{n+1}(x)$.

On differentiating the expression

$$\triangle_n(x) = (J_n(x))^2 - J_{n+1}(x)\,J_{n-1}(x) \tag{5}$$

twice, we get

$$\frac{d}{dx}\triangle_n(x) = \frac{2}{x}J_{n+1}(x)\,J_{n-1}(x) \tag{6}$$

and

$$\frac{d^2}{dx^2}\triangle_n(x) = \frac{2}{x}J_{n+1}(x)\frac{d}{dx}J_{n-1}(x) + \frac{2}{x}J_{n-1}(x)\frac{d}{dx}J_{n+1}(x) - \frac{2}{x^2}J_{n+1}(x)\,J_{n-1}(x). \tag{7}$$

Let $0 < x_{1,s} < x_{2,s} < \ldots$ denote the zeros of $J_s(x)$ in the ascending order. From (7) we see that

$$\left(\frac{d^2}{dx^2}\triangle_n(x)\right)_{x=x_{r,n-1}} = -4n\left\{\left(\frac{1}{x}J_n(x)\right)^2\right\}_{x=x_{r,n-1}} < 0$$

and

$$\left(\frac{d^2}{dx^2}\triangle_n(x)\right)_{x=x_{r,n+1}} = 4n\left\{\left(\frac{1}{x}J_n(x)\right)^2\right\}_{x=x_{r,n+1}} > 0.$$

Hence the theorem.

The statement in the above theorem is reversed if $n < 0$. In what follows we assume that $n > 0$.

If we denote the successive relative maxima of $\triangle_n(x)$ by $M_{1,n}$, $M_{2,n}$, ... and the successive relative minima by $m_{1,n}$, $m_{2,n}$, ... respectively, we have

$$M_{r,n} = \triangle_n(x_{r,n-1}) = (J_n(x_{r,n-1}))^2, \tag{8}$$

and

$$m_{r,n} = \triangle_n (x_{r,n+1}) = \left(J_n (x_{r,n+1})\right)^2. \tag{9}$$

We may also observe incidentally that

$$m_{r,n-1} = \left(J_{n-1} (x_{r,n})\right)^2 = \left(J_{n+1} (x_{r,n})\right)^2 = M_{r,n+1}.$$

Since the quantities $M_{r,n}$ and $m_{r,n}$ are positive for all values of n, it follows that

$$\triangle_n (x) > 0 \tag{10}$$

which is Turán's inequality for the Bessel function $J_n (x)$.

THEOREM 2: The sequences of relative maxima and relative minima of $\triangle_n (x)$ are decreasing beyond a certain value of r. More specifically

$$M_{r,n} > M_{r+1,n} \quad \text{if} \quad x_{r,n-1} > \xi = \sqrt{2n(n-2)}$$

and

$$m_{r,n} > m_{r+1,n} \quad \text{if} \quad x_{r,n+1} > \eta = \sqrt{2n(n+2)}.$$

If $0 < n \leq 2$, we define $\xi = 0$.

Consider the function

$$f(x) = \triangle_n (x) + \frac{2n}{x^2} \left(J_{n-1} (x)\right)^2.$$

Then, by differentiation we get

$$f'(x) = \frac{2}{x} J_{n+1} (x) J_{n-1} (x) - \frac{4n}{x^3} \left(J_{n-1} (x)\right)^2 + \frac{4n}{x^2} J_{n-1} (x) \frac{d}{dx} J_{n-1} (x)$$

$$= \frac{2}{x^3} \left(2n(n-2) - x^2\right) \left(J_{n-1} (x)\right)^2$$

so that $f(x)$ is increasing in $0 < x < \xi$ and decreasing in $x > \xi$. Also at the relative maxima of $\triangle_n (x)$, $f(x) = \triangle_n (x)$ and hence the assertion that $M_{r,n} > M_{r+1,n}$ if $x_{r+1,n-1} > x_{r,n-1} > \xi$. To prove the corresponding result for the relative minimum, consider the function

$$g(x) = \triangle_n (x) - \frac{2n}{x^2} \left(J_{n+1} (x)\right)^2.$$

Differentiating this we have

$$g'(x) = \frac{2}{x^3} \left(2n(n+2) - x^2\right) \left(J_{n+1} (x)\right)^2$$

so that $g(x)$ is decreasing in $x > \eta$. Since $g(x)$ coincides with $\triangle_n(x)$ at all the relative minima of $\triangle_n(x)$, it follows that $m_{r,n} > m_{r+1,n}$ if $x_{r+1,n+1} > x_{r,n+1} > \eta$.

This completes the proof of the theorem.

THEOREM 3: The r-th relative maximum of $\triangle_n(x)$ is greater than the r-th relative minimum, *i.e.*, $M_{r,n} > m_{r,n}$.

We have $\triangle_n(x_{r,n-1}) = M_{r,n}$ and $\triangle_n(x_{r,n+1}) = m_{r,n}$ and $(d/dx)\triangle_n(x) = (2/x) J_{n+1}(x) J_{n-1}(x)$. From the interlacing properties of the zeros of Bessel functions we know that[6, 7]

$$x_{r-1,n+1} < x_{r,n-1} < x_{r,n} < x_{r,n+1} < x_{r+1,n-1}.$$

Hence in the interval $(x_{r,n-1}, x_{r,n+1})$, Sgn $(d/dx)\triangle_n(x) = (-1)^{2r-1} = -1$, so that $\triangle_n(x)$ is decreasing in the interval and $\triangle_n(x_{r,n-1}) > \triangle_n(x_{r,n+1})$ or $M_{r,n} > m_{r,n}$ which proves the theorem.

By employing the functions $f(x)$ and $g(x)$ already introduced, we can show further that

$$M_{r,n} > \left(1 + \frac{8n^3}{x^4_{r,n+1}}\right) m_{r,n} \quad \text{if} \quad x_{r,n-1} > \xi$$

and

$$M_{r,n} > \left(1 - \frac{8n^3}{x^4_{r,n-1}}\right)^{-1} m_{r,n} \quad \text{if} \quad x_{r,n-1} > \eta.$$

THEOREM 4: For a fixed value of r, the r-th relative maxima of $\triangle_n(x)$ form a sequence of decreasing functions of n, *i.e.*, $M_{r,n} > M_{r,n+1}$. We have already noticed that $\triangle_n(x_{r,n-1}) = M_{r,n}$. We may see easily that $M_{r,n+1} = \triangle_{n+1}(x_{r,n}) = \triangle_n(x_{r,n})$. Also from the relation $(d/dx)\triangle_n(x) = (2/x) J_{n+1}(x) J_{n-1}(x)$, it follows that in the interval $(x_{r,n-1}, x_{r,n})$, Sgn $(d/dx)\triangle_n(x) = -1$, so that $\triangle_n(x)$ is decreasing in the interval and $\triangle_n(x_{r,n-1}) > \triangle_n(x_{r,n})$. Whence the theorem.

Analogously for the relative minima, we have

THEOREM 5: For a fixed value of r, the r-th relative minima of $\triangle_n(x)$ form a sequence of decreasing functions of n, *i.e.*, $m_{r,n} > m_{r,n+1}$.

We have noticed earlier that $m_{r,n-1} = M_{r,n+1}$. Combining this with the result of the previous theorem, we see that $m_{r,n-1} > m_{r,n}$ which proves the assertion.

References

1. Otto Szász .. "Inequalities concerning ultraspherical polynomials and Bessel functions," *Proceedings of the American Mathematical Society*, 1950, **1**, 256–67.

2. Watson, G. N. .. *A Treatise on the Theory of Bessel Functions*, 2nd Edition, Cambridge, 1948, p. 152.

3. Thiruvenkatachar, V. R. and Nanjundiah, T. S. "Inequalities concerning Bessel functions and orthogonal polynomials," *Proc. Ind. Acad. Sci.*, 1951, **33 A**, 373–84.

4. Otto Szász .. "On the relative extrema of the Hermite orthogonal functions," *Jour. Ind. Math. Soc.* (*N.S.*), 1951, **15**, 129–34.

5. Lakshmana Rao, S. K. .. "On the relative extrema of the Turán expression for the general Hermite function," *Indian Institute of Science Golden Jubilee Research Volume*, 1959, pp. 200-04.

6. Watson, G. N. .. "Ref. (2) above, p. 480.

7. Gray, A., Mathews, G. B. and MacRobert, T. M. *A Treatise on Bessel Functions*, 1952, p. 242.

PHOTOELECTRON SCINTILLATION SPECTROMETER AND THE CONVERSION COEFFICIENT OF THE 279 Kev. TRANSITIONS IN Tl^{203}

By B. N. Subba Rao

(*Tata Institute of Fundamental Research, Bombay-5, India*)

Received December 3, 1961

(Communicated by Dr. B. V. Thosar, F.A.SC.)

Introduction

Organic crystal scintillation spectrometers are commonly used for β-ray spectrometry where moderate resolution in energy is sufficient for the purpose. However, its utility in γ-ray spectrometry is limited by the main mode of interaction being the compton effect which gives rise to a continuous pulse height distribution.

A photoelectron spectrum of γ-rays from a suitable converter allows one to obtain monoenergetic electron lines from which one can determine the energy of the γ-ray with an accuracy comparable with that of the conversion electron line. However, the intensity of γ-rays cannot be measured with the same accuracy because of the energy dependent angular distribution of photoelectrons with respect to the direction of the incident γ-ray.

It is the purpose of this paper to describe a new possible method in which a combination of the photoelectron spectrum and the electron spectrum with the organic crystal scintillation spectrometers is employed to measure conversion coefficients and in suitable cases, relative intensities of γ-rays. Such a combination will be called in the following the photoelectron scintillation spectrometer.

The recent report (Ramaswamy, 1950) of a discrepancy between the conversion coefficients, derived by the magnetic spectrometric method (0·159) and by the scintillation spectrometric method (0·195) for the 279 Kev. transition in Tl^{203}, aroused the interest in checking the possible existence of a systematic error in the scintillation spectrometric method compared with the magnetic spectrometric one which has often been suspected (Subba Rao, 1960).

Principle of the Photoelectron Scintillation Spectrometer

The distribution of photoelectrons relative to the angle θ between the direction of propagation of the incident photon and the photoelectron released is indicated in Fig. 1 (*b*). This distribution is based on Sauter's relativistic equation* (Heitler, 1955) with the modification that in view of the rather low energy photons expected to be met with in experiments, photoelectron energy is considered in the present derivation to be $(h\nu - E_i)/m_0c^2$ instead of $h\nu/m_0c^2$ as in the original one, $h\nu$ and E_i being the photon energy and the binding energy of the electron in the i-th shell. Though experimental verification is as yet inadequate, the effect of the azimuthal (ϕ) distribution of photoelectrons is taken on theoretical grounds (Heitler, 1955) to be negligible in the following. If a suitable converter material can be chosen such that $h\nu > 2E_i$, the probability of emission of photoelectrons into the backward hemisphere is very much reduced [Y in Fig. 1 (*b*); X corresponds to $h\nu < 2E_i$]. It is to be noted that the multiple scattering effects which would further distort the pattern of angular distribution of photoelectrons in the converter do not affect the intensity measurements in the experimental arrangement described below. With the restrictions of absorption of photoelectrons in the converter, one can employ fairly thick photoelectron converters in order to obtain higher photoelectron yield. Further, such a choice ($h\nu > 2E_i$) of the converter material also results in the photoelectrons having enough energy so that absorption losses are minimised.

$$J(\theta) = \frac{\sin^2\theta}{(1-\beta\cos\theta)^4} + \frac{1}{2}\frac{3(1-\sqrt{1-\beta^2})-2\beta^2}{(1-\beta^2)^{3/2}}\frac{\sin^2\theta}{(1-\beta\cos\theta)^3},$$

in which

$$\beta^2 = \left[\frac{\frac{h\nu - E_i}{m_0c^2}\left(\frac{h\nu - E_i}{m_0c^2}+1\right)+\frac{h\nu - E_i}{m_0c^2}}{\left(\frac{h\nu - E_i}{m_0c^2}+1\right)^2}\right].$$

From these considerations, an arrangement to study the photoelectron spectrum was arrived at [Fig. 1 (*a*)]. It consists of an anthracene crystal $\frac{1}{2}''$ dia. $\times\frac{1}{4}''$ thick with a well of depth of $\frac{1}{8}''$, covered with a 150 μ gm./cm.^{2} aluminium reflector. The source is placed over a $\frac{1}{8}''$ thick lead and 1/16″ copper collimating rings in a perspex source mount with a well-defined position for the source holder. The photoelectron converter is placed in the well of the crystal. The source-converter geometry is fixed and is such

*Note.—Sauter's formula for angular distribution of photoelectrons is taken finally in the form:

that when the converter is removed electrons can be detected in the same geometry. Source-crystal distance is about 7 mm. so that the effect of electron scattering in air is not very significant for electrons of energy greater than 60 Kev.

In Fig. 1 are shown the internal conversion spectrum, the photo-electron spectrum and the compton background of the 661 Kev. transition

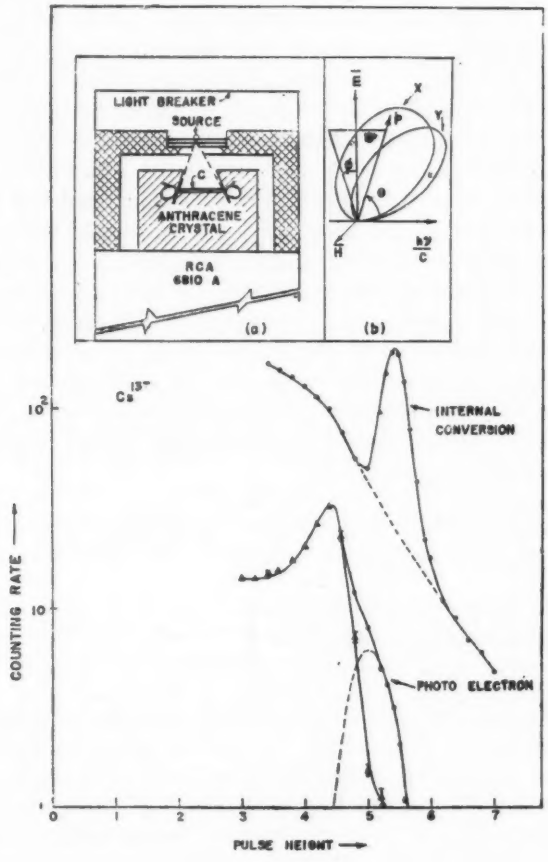

FIG. 1

in Ba^{137}. All these spectra were taken with the same source and source-detector geometry. Photoelectron spectrum was taken with a 19·2 mgm./cm.^{2} gold-converter placed in the well of the anthracene crystal. Compton

background was determined by replacing the copper collimating ring with a copper disc of the same thickness (1/16″). Adopting the photoelectric absorption coefficients due to White (1953) the total conversion coefficient obtained by comparing the areas under the internal conversion line and the photoelectron line is $\alpha = 0{\cdot}115 \pm 0{\cdot}007$. Adopting $K/L + M = 4{\cdot}6$, $\alpha^K = 0{\cdot}092 \pm 0{\cdot}01$ is obtained. This is in good agreement with the earlier measurements by other methods (Strominger, Hollander and Seaborg, 1958).

CONVERSION COEFFICIENT OF THE 279 KEV. TRANSITION IN Tl^{203}

Hg^{203} produced by the neutron irradiation in APSARA (INDIA) for two weeks of spectroscopically pure Hg_2O_3 was used as the source. The following measurements were made 72 days after irradiation.

In order to minimise the compton background without any loss in electron detection efficiency, a thinner anthracene crystal ($\frac{1}{2}$″ dia. $\times \frac{1}{8}$″ thick) with a well (1/16″ deep and 3/8″ dia.) was employed. The rest of the arrangement was as described earlier. The internal conversion lines were separated from the gross electron spectrum [Fig. 2 (*a*)] by first subtracting the compton background [Fig. 2 (*b*)] under this and then subtracting the continuous β-spectrum. With the energy calibration remaining the same in all these observations, the true β-background was obtained by first obtaining the β-spectrum in coincidence with the photopeak of the 279 Kev. γ-ray and then normalizing this coincidence β-spectrum at the maximum intensity point of the gross electron spectrum from which the Compton background had been subtracted. The resulting conversion line is indicated in Fig. 2 (*a*). The (L + M....) part of the internal conversion line tails off at the higher energy end. This is attributed to the simultaneous detection of β-particles and the conversion electrons in coincidence with them. This is possible since the mean life of the excited state in Tl^{203} is about 5×10^{-10} secs. and the overall detector resolution time is about 2×10^{-7} secs. In order to take into account the conversion electrons removed from the main peak by this process, the area under the whole conversion line including the tailing part was employed and the total conversion coefficient (α) was determined. However, assuming a gaussian distribution for the K-conversion line, $K/L+M = 2{\cdot}4$ was obtained. This is in good agreement with the value of 2·7 obtained by magnetic spectrometric measurements. This indicates the correctness of the above procedure.

The photoelectron spectrum obtained with a 28 mgm./cm.^{2} lead converter is shown in Fig. 2 (*b*). In Fig. 1 as well as in Fig. 2, all points

include statistical errors. Since the photoelectron and internal conversion lines were obtained with the same source and in the same geometry, the total conversion coefficient α is deduced from the relation,

$$\alpha = \frac{N_e}{N_p} \cdot \frac{N}{N'} \frac{\epsilon_p}{\epsilon_e} \epsilon_e \frac{\omega_\gamma}{\omega_e} = \frac{N_e}{N_p} \cdot \epsilon_p,$$

where $N = N'$ (same source), $\epsilon_e = \epsilon_e'$ (same electron detection efficiency of nearly 100%), $\omega_e = \omega_\gamma$ (same geometry) and N_e and N_p are the conversion electron and photoelectron line intensities and ϵ_p is the photoelectric conversion efficiency for lead. Thus $\alpha = 0{\cdot}205$ was obtained as an average

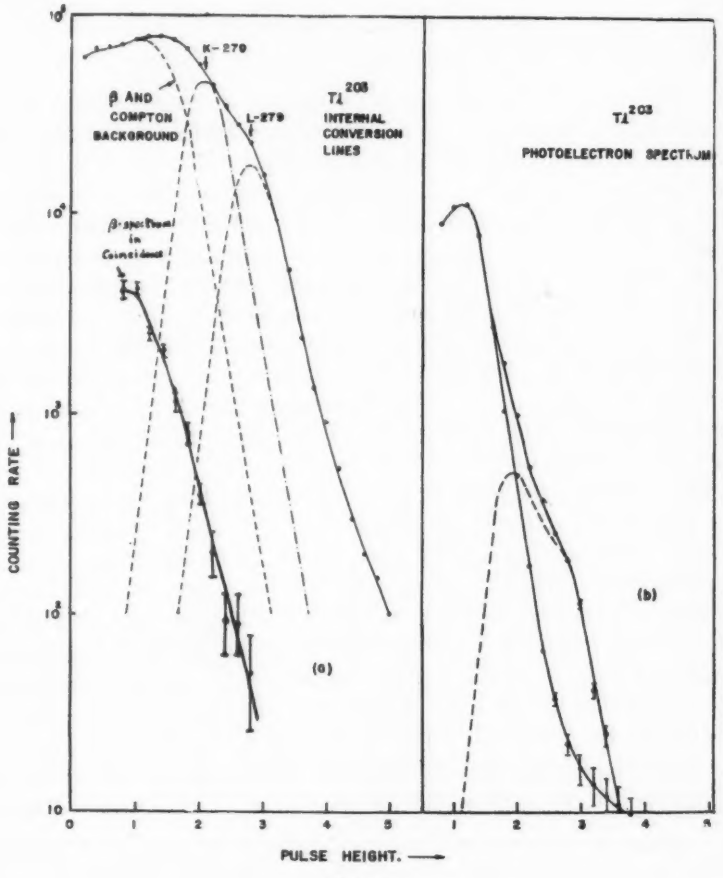

FIG. 2

of two runs after correcting for absorption of photoelectrons in the lead converter and employing the calculated (White) photoelectric cross-sections. With $K/L+M = 2{\cdot}7$, $\alpha^K = 0{\cdot}15 \pm 0{\cdot}02$ is obtained. This error is three times the mean deviation in the average value so that any possible systematic errors in subtraction of backgrounds, normalization of β-spectrum or uncertainties in the theoretical photoelectric cross-section are taken into account. This value is in agreement with the magnetic spectrometric value of $0{\cdot}159 \pm 0{\cdot}004$. Thus, the photoelectron scintillation spectrometer can be useful in the determination of conversion coefficients by a very simple and direct procedure. Where uncertainties due to background can be reduced still further, quite accurate results may be expected.

The conversion coefficient of this transition was redetermined by employing a $1\frac{1}{2}'' \times 1\frac{1}{2}''$ NaI (Tl) crystal and a point source placed at a distance of 9·6 cm. from the crystal along the axis of the crystal. The source holder was held in position by an insulation tape which was fixed at the two ends 1 yard apart. The crystal was provided with a graded shield consisting of lead, cadmium and brass and there was no material within 3 yards in front of the crystal. Thus background and scattered radiation were reduced considerably. The background below X-ray peak was inferred by suppressing the X-rays by means of a 100 mgm./cm.^{2} tin-absorber placed midway between the source and detector [Fig. 3 (*a*)]. This background, consisting mainly of compton distribution and the back-scattered peak, is shown by dashed lines. Background under the spectrum without the source has been subtracted from the spectra [Fig. 3 (*b*)] I & II. After corrections for absorption in the material surrounding the crystal and taking into account the efficiency of detection (Wolicki and others) $\alpha^K = 0{\cdot}153 \pm 0{\cdot}012$ was obtained. Since in this method α^K is deduced from the relation

$$\alpha^K = \frac{N_X}{N_\gamma} \frac{\epsilon_X}{\epsilon_\gamma} \frac{\Omega_X}{\Omega_\gamma} \frac{1}{\omega_K},$$

with the fairly well-known values of the K-fluorescence yield ω_K and detection efficiencies ϵ_X and ϵ_γ and with the solid angle of detection being the same ($\Omega_X = \Omega_\gamma$) the large deviations could arise mainly through the X- and γ-ray intensities. This can happen if either the background under the X-ray peak is uncertain or there is some extraneous contribution to the X-ray region. It is not obvious how the same method could lead to results different from those of earlier workers by the scintillation spectrometric method (Ramaswamy, 1960). This has been repeated three times and all of them agree with the value $0{\cdot}153 \pm 0{\cdot}012$.

However, it appears relevant to point out that the spectra studied only a fortnight after irradiation of the source-sample lead to a result $\alpha^K = 0{\cdot}25 \pm 0{\cdot}02$ in spite of the fact that the Hg^{197} activity which contributes mostly to this X-ray region had undergone a decay for nearly five half-lives. This result was obtained by the same method as described above.

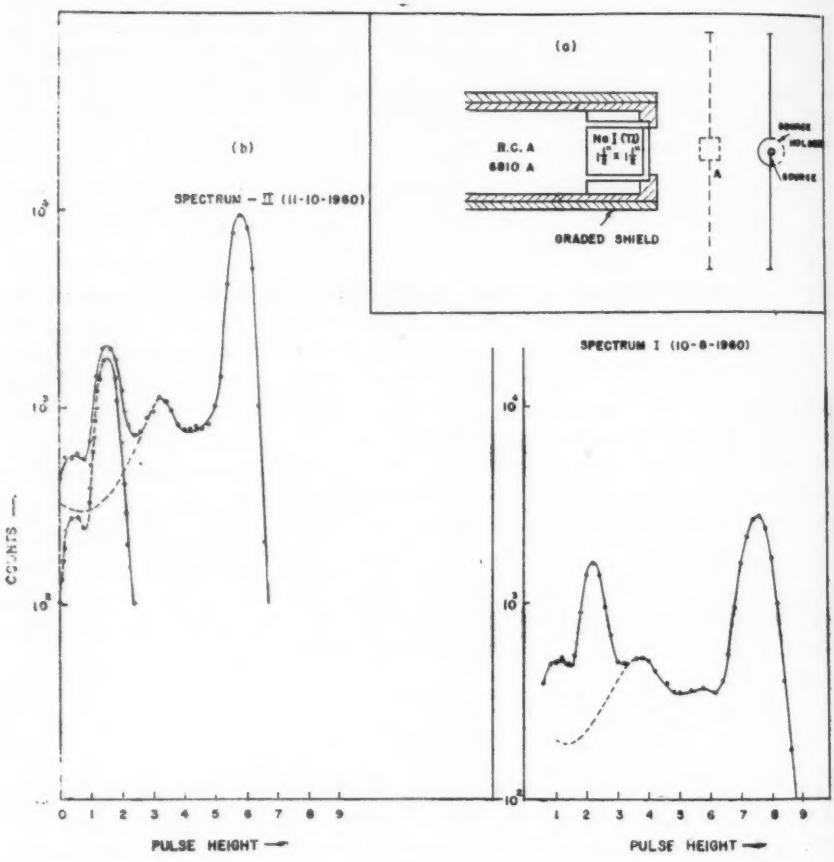

FIG. 3

From these measurements, it is concluded that scintillation spectrometric methods do not indicate any systematic errors compared with magnetic spectrometric method (Nordling *et al.*, Wapstra and Nijgh, 1957) in the case of the 279 Kev transition in Tl. [203]

Summary

An experimental arrangement combining the photoelectron and organic crystal scintillation spectrometer methods, called a photoelectron-scintillation spectrometer, is described and its utility in making direct measurements of conversion coefficients without a specific knowledge of source-strength, source-detector geometry, efficiency of detection and the energy dependent angular distribution effects and multiple scattering effects, is described.

By this method and the conventional method of measuring X- and γ-ray intensities with NaI (Tl) crystal, the conversion coefficients of the 279 Kev. transition in Tl^{203} are found to be $\alpha^K = 0{\cdot}15 \pm 0{\cdot}02$ and $\alpha^K = 0{\cdot}153 \pm 0{\cdot}012$, respectively. These values indicate that there are no systematic errors in the scintillation spectrometric methods as compared to the magnetic spectrometric results in this case.

The author is much indebted to Dr. B. V. Thosar for some helpful discussions.

References

1. White, G. .. *Natl. Bur. Standards Report No.* 2763, 1953.
2. Wolicki and others .. *Naval Research Laboratory Report*, pp. 4833.
3. Heitler, W. .. *Quantum Theory of Radiation*, 1955.
4. Wapstra and Nijgh .. *Nucl. Phys.*, 1956, **1**, 245.
5. Nordling *et al.* .. *Ibid.*, 1956, **1**, 326.
6. Strominger *et al.* .. *Revs. Mod. Phys.*, 1958, **30**, 585.
7. Ramaswamy and Jastram .. *Nucl. Phys.*, 1960, **15**, 510.
8. Subba Rao, B. N. .. *Nuovo Cimento*, 1960, **17**, 189.

THE SIGNIFICANCE OF THE PHASE SYNTHESIS

By R. Srinivasan

(*Department of Physics, University of Madras, Madras* 25, *India*)

Received April 15, 1961

(Communicated by Dr. G. N. Ramachandran, F.A.Sc.)

ABSTRACT

This paper gives an account of the results of the tests that have been carried out to assess the relative importance of the phase angles and structure amplitudes in a Fourier synthesis. For this, the phase factors, $e^{i\alpha}$, have been combined in different ways with structure amplitudes such as when the latter are (*a*) replaced by the r.m.s. of the structure amplitudes (*i.e.*, by $\sqrt{\Sigma f_i^2}$), (*b*) randomly chosen from the set of correct structure amplitudes, (*c*) made us much anti-correlated (about the mean) with the correct ones as possible and (*d*) taken to be those of an entirely different structure. The above syntheses which are only modifications of the phase synthesis, $e^{i\alpha}$, have been tested on both the centrosymmetric and non-centrosymmetric projections of a known structure. They strongly establish the greater importance of the phase angles in a Fourier synthesis.

1. Introduction

In a series of papers from this laboratory (Ramachandran and Raman, 1959; Raman, 1959; Raman, 1960; Srinivasan, 1960 *a*; Srinivasan and Aravindakshan, 1960; hereafter referred to as Parts I, II, III, IV and V respectively) the problem of deconvoluting the Patterson function when a part of the structure is known, was considered in detail. In the course of these studies it became necessary to analyse the significance of the standard syntheses which employ for their Fourier coefficients various standard functions of F, such as $|F|$, $e^{i\alpha}$, $1/F$, etc. It was pointed out in Part I and later proved in a more rigorous way in Parts II and IV that the phase synthesis $e^{i\alpha}$ resembles closely the Fourier synthesis while the modulus synthesis, $|F|$, resembles the Patterson. Though this indicated in a general way the importance of the phase angles, a closer study of the relative importance of the phase angles and the structure amplitudes was thought worthwhile. The results of such a study are presented in this paper.

2. Description of the Various Syntheses

The calculations were all made on the centrosymmetric and non-centrosymmetric projections of L-tyrosine hydrochloride whose structure has been thoroughly analysed in this laboratory (Srinivasan, 1959). The crystal data of this compound are: $a = 11{\cdot}1$, $b = 9{\cdot}1$, $c = 5{\cdot}1$A, $\beta = 92°$, two molecules of $C_9H_{12}NO_3.HCl$ per cell, space group $P2_1$. In all the syntheses to be described below the phase angles referred to (or the signs in the centrosymmetric case) correspond to those calculated for the above structure (Srinivasan, 1959) unless otherwise stated.

(*a*) *The Normalised Phase Synthesis.*—To start with, a modified form of the phase synthesis, $e^{i\alpha}$, was devised. The modification consisted in not using unit amplitudes for all reflections as in $e^{i\alpha}$, but a value equal to $\sqrt{\Sigma f_j^2}$ which is the mean for all reflections having the same value of (sin θ/λ). Thus, in effect, the magnitudes of the geometrical structure factors of all reflections were made equal, but all of them were multiplied by a mean atomic scattering factor. We shall call this synthesis the "normalised phase synthesis", the normalisation being done such that $\Sigma \mid F \mid^2$ is the same for this synthesis and the Fourier synthesis. The syntheses for the non-centrosymmetric and the centrosymmetric projections are shown in Figs. 1 (*b*) and 2 (*b*) respectively along with the actual Fourier syntheses in Figs. 1 (*a*) and 2 (*a*).

In carrying out the calculations the value of $\sqrt{\sum_j f_j^2}$ for each reflection was obtained from a graph. The temperature factor was also applied to the amplitudes and it was the same as that employed for the actual crystal. It will be noticed that the agreement between the normalised syntheses [Figs. 1 (*b*) and 2 (*b*)] and the actual Fourier syntheses [Figs. 1 (*a*) and 2 (*a*)] is extremely good.

(*b*) *The Random Phase Synthesis.*—The interesting question now arises as to what would happen if random values of $\mid F \mid$ are used along with the correct phase angles, but not equal values (apart from the '*f*' factor variation) as in the above synthesis. Such a synthesis which may be called the "random synthesis" was calculated. However, in order to ensure the same statistical distribution of structure amplitudes as in the correct structure, the reflections were grouped into various ranges of (sin θ/λ) and in each range the values of the actually observed $\mid F_0 \mid$'s (Srinivasan, 1959) were randomly permuted amongst themselves and these were then used with the correct phase angles to calculate the synthesis. The syntheses for the non-centrosymmetric and the centrosymmetric cases are given in Figs. 1 (*c*) and 2 (*c*) respectively.

Surprisingly, even in these random syntheses, the structure is revealed in fairly good detail.

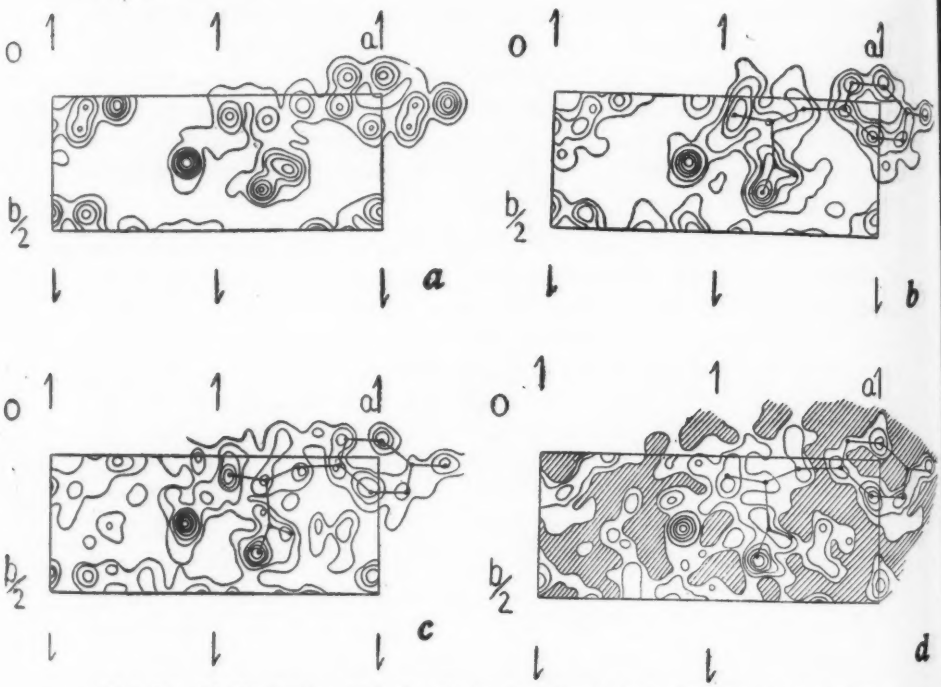

FIG. 1*. (*a*) The Fourier synthesis, (*b*) the normalised phase synthesis, (*c*) the random phase synthesis and (*d*) the anti-correlated phase synthesis of L-tyrosine hydrochloride projected down the *c*-axis. Contours are at intervals of $2e/A^2$ at chlorine and $1e/A^2$ elsewhere, starting from $2e/A^2$.

* The different kinds of atoms in the molecule of tyrosine are not marked in all the figures but only in Figs. 3 (*b*) and 4 (*b*) where small dots correspond to carbons big dots to oxygens and open circle to nitrogen.

(*c*) *The Anti-correlated Phase Synthesis.*—Now, it was thought worthwhile to go a step further and take the strong reflections weak and *vice versa.* This would be equivalent to making the new set of amplitudes and the correct set as much anti-correlated about their mean as possible.* The method adopted for getting the *maximum* anti-correlation was as follows: In each range of $(\sin\theta/\lambda)$ the various reflections were arranged in decreasing order of magnitude. The whole sequence was now inverted so that the

* For a proper explanation of the various statistical terms used in the discussion *see* Appendix I.

strongest reflection would become the weakest and so on. However, it will not be possible to realise perfect anti-correlation about the mean by this process. The possibility of achieving this depends on the nature of the probability function and it can be shown that, unless the function is symmetrical about the mean, perfect anti-correlation is not possible. In our present case, the probability functions for the centrosymmetric and non-centrosymmetric cases are not symmetrical about the mean (Ramachandran and Srinivasan, 1960) and hence perfect anti-correlation cannot be realised for them. However, the maximum possible anti-correlation for any type of distribution can be worked out and they are given in Appendix I for the centrosymmetric and non-centrosymmetric cases. The theoretical maximum of $-0{\cdot}89$ for the non-centrosymmetric case agrees fairly well with the value of $-0{\cdot}75$ as calculated from the actual data used for the anti-correlated synthesis. The difference between the two is to be expected since the procedure adopted is subject to the same types of errors as are encountered in the calculation of a Wilson plot. The synthesis was calculated only for the non-centrosymmetric projection and is shown in Fig. 1 (*d*). It is very surprising indeed to find that even this diagram shows the structure in good detail.

3. Explanation of the Syntheses

(*a*) *From the Fourier Point of View.*—The normalised phase synthesis confirms the most essential property of the phase synthesis deduced theoretically in Parts II and IV, namely, that it resembles closely the Fourier synthesis. The consequence of taking $\sqrt{\Sigma f_j^2}$ for the coefficients instead of unit amplitudes as in $e^{i\alpha}$ will be that peaks will not be sharp but will have a finite size and shape corresponding to an average atom in the structure. The normalisation also makes it possible to compare directly this synthesis with the actual Fourier synthesis. It is interesting to see that *even the relative strengths of carbon, oxygen and chlorine have come out correctly*, even though the amplitudes fed in correspond to those of a single average atom in the unit cell.

It will be noticed that the random synthesis is also almost as good as the normalised phase synthesis though it contains some spurious peaks as compared with the practically uniform background in the latter. That the random synthesis would reveal the structure in such good detail could not have been anticipated to start with. In fact, it was this rather unexpected result that suggested the next test that was made, namely, to use a set of amplitudes completely anti-correlated with the correct ones. The resultant synthesis, Fig. 1 (*d*), is of course worse than the random synthesis, but still

the tyrosine molecule is clearly discernible. What is more interesting is that the relative strengths of the peaks at the positions of chlorine, carbon, etc., are practically unaffected. However, the number of spurious peaks is now somewhat larger as compared with the random synthesis and their strengths are also larger.

The real reason why even under these diverse conditions the phase synthesis is able to reveal the structure can be understood by making a closer study of the problem. The explanation follows essentially from the general idea of the deconvolution of the Patterson function and of the principle of modulation of one structure by another (Parts I and II). All the above syntheses can be interpreted as the modulation of the appropriate modulus synthesis with the phase synthesis, $e^{i\alpha}$. The latter is practically same as the Fourier synthesis and contains first order peaks of strengths $0{\cdot}90f_i/S_N$ at the same positions as in Fourier where $S_N = \sqrt{\sum_j f_j^2}$ (Part IV). Now, because of the fact that the structure amplitudes used in the case of random and the anti-correlated syntheses do not correspond to any actual " structure", their modulus synthesis would not contain only positive peaks as in a modulus synthesis of any real structure (Part IV). However, at the origin alone both

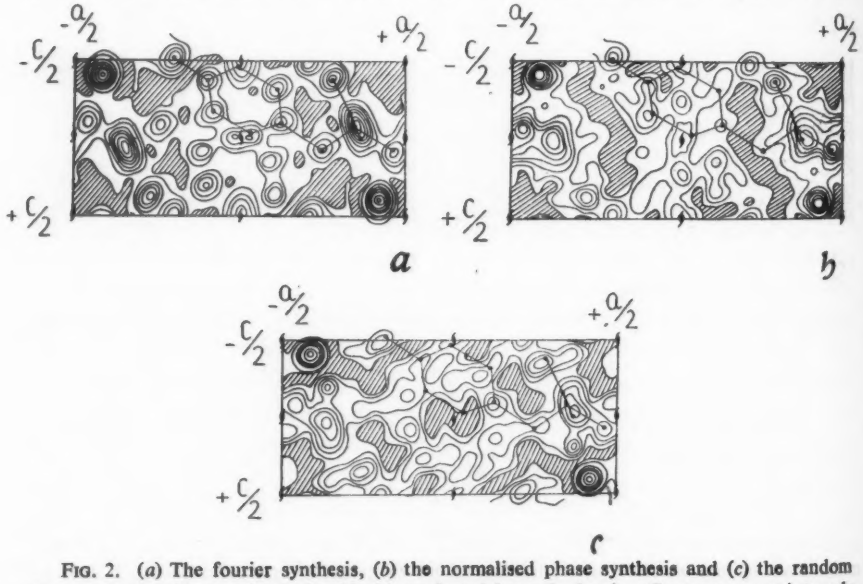

FIG. 2. (*a*) The fourier synthesis, (*b*) the normalised phase synthesis and (*c*) the random phase synthesis of L-tyrosine hydrochloride projected down the *b*-axis. Contours are at intervals of $2e/A^2$ at chlorine and $1e/A^2$ elsewhere, starting from $3e/A^2$. Shaded area corresponds to less than $3e/A^2$.

these will have a strength equal to that of the actual modulus synthesis. Elsewhere, one would expect a fluctuating background. The only strong interactions which arise in the modulation of this synthesis with the phase synthesis will therefore correspond to those of an origin peak with the first order peaks of the phase synthesis and will thus lead to the structure contained in the phase synthesis, *i.e.*, at the correct atomic positions.

Another general feature that might be observed in Figs. 1 and 2 is that the phase synthesis for the non-centrosymmetric case is distinctly better than that for the centrosymmetric case. This result is best understood after we consider another interesting aspect of the problem, namely, from the statistical point of view.

(*b*) *From the Statistical Point of View.*—The terms random and anti-correlated have been used in the previous sections in relation to the mean of the distribution. These would have conveyed the idea that the distributions chosen are not correlated or anti-correlated to the distribution of the structure amplitudes for the correct structure. However, it should be remembered that in a Fourier synthesis it is the actual structure amplitudes that is employed so that the correlation about the mean (k) is not so important as the direct correlation (c). The terms correlation about the mean and the direct correlation are explained in Appendix.

If Table I of Appendix is examined it will be seen that the direct correlation between the structure amplitudes of the assumed distribution and the actual distribution is as high as 0·79 for the non-centrosymmetric case and 0·63 for the centrosymmetric case when these are randomly correlated about the mean. Consequently, it is not at all surprising that the random synthesis reveals much of the details of the actual structure. Even when the two sets of structure amplitudes are anti-correlated (or as much anti-correlated as possible) the direct correlation coefficient is still as high as 0·60 for the non-centrosymmetric case. In this case, even the anti-correlated synthesis does reveal the structure quite well and this becomes understandable from the magnitude of the direct correlation coefficient. The correlation is poorer in the centrosymmetric case (about 0·40) but it is believed it is good enough to reveal some details of the structure.

The large value of the direct correlation arises essentially because the quantity $|F|$ is always positive. Consequently, even if there are variations about the mean there is always a positive cerrelation between the absolute magnitudes in the two sets of the data because both of them must necessarily be positive.

It will be noticed from Table I that the direct correlation for the non-centrosymmetric case is systematically larger than that for the centrosymmetric case for all the different types of syntheses. This explains the fact already mentioned, namely that the phase synthesis for the non-centrosymmetric case is distinctly better than that for the centrosymmetric case, as a general feature.

4. TESTS ON A LIGHT-ATOM STRUCTURE

(*a*) *The Normalised Phase Synthesis.*—It will be observed that all the above syntheses have been calculated for the compound L-tyrosine hydrochloride which is not a purely light-atom structure. Hence the theoretical considerations given above are not strictly applicable to this case. The effect of the presence of heavy atom on the distribution function P(*y*) has already been worked out (Srinivasan, 1960 *b*). In the present case, in which there are two heavy atoms in the unit cell, the general tendency is to alter the distribution curve for both centrosymmetric and non-centrosymmetric cases such that there are a large number of reflections having their value near the mean. The effect of this in both cases, is to make the value of *c* larger (*see* Appendix I) than if the heavy atoms were not present. In view of this fact, it was felt that the test should be carried out on a pure light-atom structure. This was actually done and the normalised phase synthesis for both the non-centrosymmetric and centrosymmetric cases were calculated for the structure "tyrosine" alone obtained by removing the two chlorine atoms from the tyrosine hydrochloride structure. The resultant syntheses [Figs. 3 (*a*) and 3 (*b*)] will be found to be practically as good as Figs. 1 (*b*) and 2 (*b*). It was therefore felt not necessary to calculate the other syntheses.

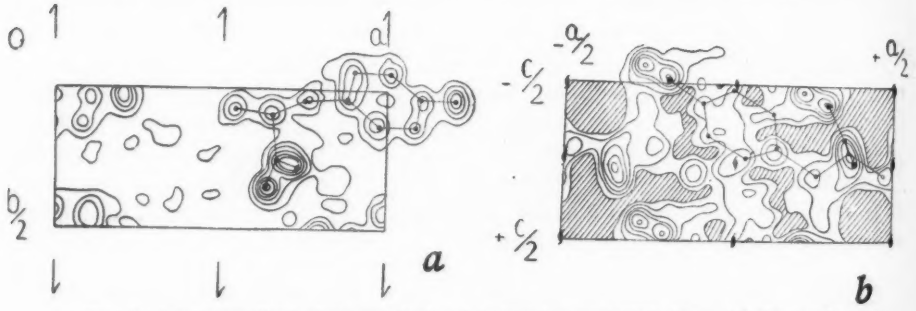

FIG. 3. The normalised phase synthesis of L-tyrosine projected down (*a*) the *c*-axis and (*b*) the *b*-axis. Contours are same as in Figs. 1 and 2 respectively.

(*b*) *Use of the Structure Amplitudes of an Entirely Different Structure.*—The results of carrying out the different types of syntheses described earlier

suggested one other interesting possibility, namely, that of combining the structure amplitudes of an actual structure with the phase angles calculated from an entirely different structure. For this purpose, six atoms were assumed at the positions marked by crosses in Fig. 4 (*a*) and these atoms were assumed to have a suitable scattering factor (actually 1·7 times the '*f*' value of carbon) falling off with θ as for a carbon atom. This was done to make the value of $\sum_j f_j^2$ of this structure (which we may call as the correct structure *A*, and denote its structure amplitudes by $|F_A|$) the same as that for the assumed structure. Now, the assumed structure (*B*) was taken to be the structure of pure tyrosine. The phase angles σ_B for tyrosine were calculated and were used along with the structure amplitudes $|F_A|$ to calculate a synthesis using $|F_A| \exp. i\sigma_B$ as Fourier coefficients. The synthesis for the non-centrosymmetric projection is shown in Fig. 4 (*a*). Figure 4 (*b*) shows the difference Fourier synthesis $(|F_A| - |F_B|) \exp. i\sigma_B$.

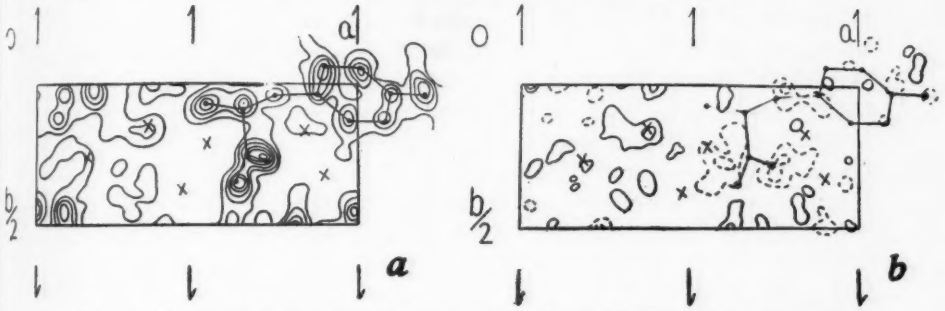

FIG. 4. (*a*) The synthesis using $|F_A| \exp.\alpha_{I_B}$ as fourier coefficients where *A* corresponde to an arbitrary six-atom structure (marked by crosses) and *B* to tyrosine. Contours are sams as in Fig. 1. (*b*) The difference synthesis, $(|F_A| - |F_B|) \exp_{I\alpha_B}$. Contours are at intervals of 1e/A^2. Positive and negative contours are shown by continuous and broken lines respectively. The zero contour is omitted.

5. DISCUSSION

The synthesis using the structure amplitudes of an arbitrary structure along with phases calculated from a different structure represents probably the extreme possible case in the present series of tests. The agreement between this synthesis [Fig. 4 (*a*)] and the Fourier [Fig. 1 (*a*) with the chlorine removed] is very good and it will be seen that all the atoms of tyrosine have come out in it. Particularly it is noteworthy that, excepting at one place, there are practically no strong peaks at the atomic positions of the arbitrary structure *A* [marked by crosses in Fig. 4 (*a*)], whose structure amplitudes were used in the synthesis. The one peak mentioned above is, however, believed to be spurious.

From this, the following important conclusion is obvious, namely, that if a Fourier synthesis is made using the amplitudes of the correct structure (A) along with the phases calculated for an assumed wrong structure (B) then the resultant synthesis would contain peaks only at the assumed positions and not at the correct positions.

This seems to be in apparent contradiction with the well-known fact in structure analysis, namely, that the correct structure is usually arrived at by a series of successive Fourier syntheses, assuming initially atoms to be present at all the prominent peaks in a trial Fourier synthesis. The resolution of this paradox follows from the general idea of modulation (Part I).

Now, the modulus synthesis, $|F_A|$, contains an origin peak of strength $0{\cdot}92\,S_N$ and non-origin peaks of strengths $0{\cdot}38 f_i f_j/S_N$ at $r_{Ai} - r_{Aj}$, while the phase synthesis, $e^{i\alpha_B}$, contains peaks of strengths $0{\cdot}90 f_i/S_N$ at r_{Bi}. The modulation of the two should obviously lead to peaks at r_{Bi} arising out of the interactions between the origin peak of the former and the first order peaks of $e^{i\alpha_B}$ at r_{Bi}. The other interactions between $r_{Ai} - r_{Aj}$ and r_{Bi} would, in general, lead only to a background and in particular there will not be any concentration of electron density at r_{Ai}. If, on the other hand, the structures A and B have some atoms in common, say P of them, then P of the peaks in r_{Bi} would be of the type r_{Aj} so that the interactions between $r_{Ai} - r_{Aj}$ and r_{Bi} will lead to concentration at r_{Ai}. The strengths of A will, of course, depend on the number of coincident atoms (P) and will, in general, be weaker than those at B.

It follows from the above that *the necessary condition for peaks to occur at the correct atomic positions,* A, *is that at least some of the atoms used for calculating the phases must coincide with those in the structure* A.

This again shows that the usual method of successive Fourier syntheses would successfully converge to the correct structure only if the assumed structure or at least part of it is near the correct one. The method would obviously fail if completely wrong positions are used, to start with. Of course, there is no reason why the phases fed in from a completely arbitrary structure should lead to the correct one since, if it were to be true, it would be an absurdly simple solution to the phase problem.

However, the fact, that the assumed structure is wrong, would easily be revealed by the R value. For a completely wrong structure it would be 83% for the centrosymmetric and 59% for the non-centrosymmetric case respectively (Wilson, 1950). Further, the difference Fourier synthesis might

also help in detecting the falsity of the structure. Even this is not so very helpful as is usually supposed. Though there is a small concentration of negative density in Fig. 4 (*b*) at some of the tyrosine atoms, both positive and negative peaks occur at random in the synthesis the maximum values corresponding approximately only to a helium atom. Probably the error synthesis would have been more useful in detecting the wrong atomic positions.

References

Ramachandran, G. N. and Raman, S. *Acta Cryst.*, 1959, **12**, 957.

—— and Srinivasan, R. .. *Ibid.*, 1959, **12**, 410.

Raman, S. .. *Ibid.*, 1959, **12**, 964.

———— .. *Ibid.*, 1960, in press.

Srinivasan, R. .. *Proc. Ind. Acad. Sci.*, 1959, **50 A**, 19.

———— .. Sent for publication. 1960 *a*.

———— .. *Acta Cryst.*, 1960 *b*, **13**, 388.

—— and Aravindakshan, C. .. *Ibid.*, 1960, sent for publication.

APPENDIX I

Correlation between Structure Amplitudes

We define the correlation between the structure factors F_1 and F_2 of two structures 1 and 2 as

$$c(F) = \frac{1}{2}\frac{\Sigma(F_1F_2^* + F_2F_1^*)}{\sqrt{\Sigma|F_1|^2}\cdot\sqrt{\Sigma|F_2|^2}} = \frac{\Sigma|F_1||F_2|\cos(\alpha_1 - \alpha_2)}{\sqrt{\Sigma|F_1|^2}\cdot\sqrt{\Sigma|F_2|^2}} \quad (1)$$

where the notation is self-explanatory. We would be mainly interested in the case when the two phase angles α_1 and α_2 are the same for any reflection so that the cosine factor in (1) becomes unity giving the following quantity which would also be called the correlation between the structure amplitudes $|F_1|$ and $|F_2|$. Thus

$$c(|F|) = \frac{\Sigma|F_1||F_2|}{\sqrt{\Sigma|F_1|^2}\ \sqrt{\Sigma|F_2|^2}}. \quad (2)$$

The term coefficient of linear correlation (k) between two statistical variates is usually used to denote the correlation about the mean. Applying this to our case, we may write k as

$$k = \frac{\Sigma(|F_1| - \overline{|F_1|})(|F_2| - \overline{|F_2|})}{\sqrt{\Sigma|F_1|^2}\ \sqrt{\Sigma|F_2|^2}}. \quad (3)$$

We shall hereafter use the term "direct correlation" to denote $c(|F|)$ as defined by (2) and the term "correlation coefficient" or simply "correlation" to denote k as defined by (3). (If it desired to be explicit we may use "correlation about the mean" to denote k.)

It is possible to express c in terms of k by expanding (3) and substituting from (2). This gives

$$c = \frac{\Sigma m_1(|F_1|)\, m_1(|F_2|) - k\sigma(|F_1|)\,\sigma(|F_2|)}{\sqrt{m_2(|F_1|)}\ \sqrt{m_2(|F_2|)}} \quad (4)$$

where σ is the standard deviation and m_1 and m_2 are the first and second moments of the variates.

In the discussion to follow we would be mainly interested in the case when the two variated have the same probability distributions so that we may take $m_1(|F_1|) = m_1(|F_2|) = m_1$ and $\sigma(|F_1|) = \sigma(|F_2|) = \sigma$, etc. Equation (4) then reduces to

$$c = k + \frac{m_1^2}{m_2}(1 - k). \quad (5)$$

When the two variates are one and the same, both k and c should be equal to unity which also follows from (5).

The values of m_1 and m_2 for the normalised structure amplitudes are well known in the case of both non-centrosymmetric and centrosymmetric distributions. These are $m_1 = (\sqrt{\pi}/2)$, $m_2 = 1$ for the former and $m_1 = \sqrt{(2/\pi)}$, $m_2 = 1$ for the latter. Substituting these values in (5) the values of c are obtained to be as in Table I. The values in brackets (where given) correspond to the actual values found in the calculation of the corresponding syntheses described in the text.

It will be seen from Table I that even for perfect anti-correlation* the value of c is quite appreciable and particularly for the non-centrosymmetric case it is quite high. Also the value of c for the non-centrosymmetric case is systematically higher than the corresponding value for the centrosymmetric case. This essentially arises because of the fact that the probability distribution function in the former case has a large number of reflections with their values clustered round the mean while in the centrosymmetric case they have a comparatively wider dispersion. Thus if we could have an ideal case of a distribution which is a delta function at the mean, the value of c would always be unity. Table I also tells us that the worst possible direct

TABLE I

Values of the direct correlation c *for different values of* k
Actually observed values are given in brackets

Distribution \ k	1·0	0·5	0·0	−0·5	−0·80*	−0·89*	−1·0
Non-centrosymmetric ..	1·0	0·89	0·79 (0·74)	0·68	..	0·59 (0·55)	0·57
Centrosymmetric	1·0	0·82	0·63 (0.69)	0·45	0·34	..	0·26

* These values correspond to the maximum possible values of the anti-correlation coefficient for the centrosymmetric and non-centrosymmetric cases respectively.

* The terms "correlated" and "anti-correlated" (about the mean) are used in general, where k is positive and negative respectively, while "perfect correlation" and "perfect anti-correlation" are used to denote the extreme cases of $k = +1$ and -1 respectively.

correlation is for a centrosymmetric structure when the structure amplitudes are perfectly anti-correlated.

However, the above discussion on the relationship between c and k is purely from a theoretical point of view and it remains a separate issue whether the case of perfect anti-correlation is at all realisable in practice for any type of distribution. In fact, it may be stated here that, unless the distribution is symmetrical about the mean, perfect anti-correlation about the mean is not possible. (The details will be presented elsewhere.) This is also equivalent to the condition that the mean and the median of the distribution should be the same. Further, it is possible to calculate the maximum value of anti-correlation attainable in practice for any type of distribution. The values for the non-centrosymmetric and the centrosymmetric distributions are mentioned in Table I. It will be noticed that this maximum value is larger for the non-centrosymmetric than the centrosymmetric case. This is understandable since the distribution for the former case is fairly symmetrical about the mean while in the latter case it is rather asymmetrical.

In conclusion, I wish to express my sincere thanks to Prof. G. N. Ramachandran for valuable suggestions during this investigation. My thanks are also due to Miss V. Valambal and Mr. S. K. Majumdar for helping me in the calculations.

290–61 Printed at the Bangalore Press, Bangalore City, by T. K. Balakrishnan, Superintendent, and Published by The Indian Academy of Sciences, Bangalore.

NOTICE TO AUTHORS

Scientific papers intended for publication in the *Proceedings of the Indian Academy of Sciences* can be accepted only when they are communicated by a Fellow of the Academy whose duty shall be to satisfy himself that such communications are fit to be read at the Meeting of the Academy and published in its *Proceedings*.

Papers should not ordinarily exceed fifty pages of foolscap. MSS. should be either typewritten or written in legible hand on one side of the paper. All papers should be carefully revised by the authors and should be absolutely in final form for printing. Position for text-figures should be indicated. Each paper shall conclude with a critical summary not exceeding 350 words.

Drawings, diagrams or other illustrations should be made on larger scale (preferably) twice the size than the ones in which they are intended to appear. They should be done in Indian ink on bristol board with lettering in pencil. Scale of magnification of camera lucida tracings should be indicated by the side of drawings. In certain special cases arrangements will also be made for monochrome lithographic and other colour plates. Reduction of illustrations desired should be indicated in pencil. Appropriate legends should accompany all drawings. Names of authors are to be marked in pencil on the left-hand corner of drawing sheets. Photomicrographs should be securely mounted with colourless paste.

All tables, quotations and footnotes which will be set hereafter (beginning from Vol. I, No. 2) in types smaller than the text, should be typewritten on separate sheets and placed with the text in proper sequence. Footnotes should be numbered in Arabic numerals.

References to literature in the text should be given, whenever possible, in chronological order, only the names of authors and years of publication, in brackets, being given. They should be cited in full after the summary, the authors' names following in alphabetical order. Thus,

Name or Names of author; Name of Journal (abbreviation) with a single underline; Year of publication; Number of Volume with a double underline, and lastly page. The following would be a useful illustration:—

Bergmann and Stather . . . . . Z. Physiol. Chem., 1926, 152, 189.

Two copies of slip-proof and wherever possible, a page proof for final revision will be sent to authors. All corrections are best made on the slip-proof which should be transmitted to the Office of the Academy. All proof corrections involve heavy expenses which would be negligible if the papers are carefully revised by the authors before submission.

Fifty free reprints including plates and with cover will be supplied for each paper. Additional copies can be supplied at cost on previous intimation.

Blocks appearing in the *Proceedings* will be available for purchase by their respective authors. Orders for the same should be sent along with the corrected proofs and in any case not later than one month after the date of publication of the paper. The price charged would be 25% of the actual cost of the blocks *plus* freight and despatching charges. If the blocks are reproduced in other journals or publications, due acknowledgment should be made in them to the *Proceedings*.

The original drawings and plates of blocks appearing in the *Proceedings* will be returned to such of the authors as may require them provided the cost of despatching such originals is borne by them.

CONTENTS

PAGE

Fluorescence and Scintillation Spectra of CsI (Tl) Crystal . . . . . R. G. Lagu and B. V. Thosar 219

A Study of the Pre-Sunrise F-Layer Stratification at Kodaikanal . . . . . B. N. Bhargava and R. V. Subrahmanyan 227

On the Relative Extrema of the Turán Expression for Bessel Functions . . . . . S. K. Lakshmana Rao 239

Photoelectron Scintillation Spectrometer and the Conversion Coefficient of the 279 Kev. Transitions in Tl^{203} . . . . . B. N. Subba Rao 244

The Significance of the Phase Synthesis . . . . . R. Srinivasan 252